

# Structure-Enhanced Protein Instruction Tuning: Towards General-Purpose Protein Understanding with LLMs

Wei Wu<sup>†</sup>

School of Artificial Intelligence and  
Data Science, University of Science  
and Technology of China  
Hefei, China  
urara@mail.ustc.edu.cn

Mingze Yin<sup>†</sup>

College of Computer Science and  
Technology, Zhejiang University  
Hangzhou, China  
12521039@zju.edu.cn

Jieping Ye

Alibaba Cloud Computing  
Hangzhou, China  
yejieping.ye@alibaba-inc.com

Chao Wang<sup>\*</sup>

School of Artificial Intelligence and  
Data Science, University of Science  
and Technology of China  
Hefei, China  
wangchaoai@ustc.edu.cn

Yiheng Zhu<sup>†</sup>

College of Computer Science and  
Technology, Zhejiang University  
Hangzhou, China  
zhuyiheng2020@zju.edu.cn

Liyi Chen<sup>†</sup>

School of Artificial Intelligence and  
Data Science, University of Science  
and Technology of China  
Hefei, China  
liyichen@ustc.edu.cn

Kun Fu

Alibaba Cloud Computing  
Beijing, China  
fukun.fu@alibaba-inc.com

Zheng Wang

Alibaba Cloud Computing  
Beijing, China  
wz388779@alibaba-inc.com

Hui Xiong

Thrust of Artificial Intelligence, The  
Hong Kong University of Science and  
Technology (Guangzhou)  
Guangzhou, China  
Department of Computer Science and  
Engineering, The Hong Kong  
University of Science and Technology  
Hong Kong SAR, China  
xionghui@ust.hk

First, we warm up the enhanced pLMs using contrastive learning and structure denoising. Then, caption-based instructions are used to establish a basic understanding of proteins. Finally, we refine this understanding by employing a mixture of experts (MoEs) to capture more complex properties and functional information with the same number of activated parameters. Moreover, we construct the largest and most comprehensive protein instruction dataset to date, which allows us to train and evaluate the general-purpose protein understanding model. Extensive experiments on both open-ended generation and closed-set answer tasks demonstrate the superior performance of SEPIT over both closed-source general LLMs and open-source LLMs trained with protein knowledge.

## CCS Concepts

- Computing methodologies → Natural language processing;
- Applied computing → Bioinformatics.

## Keywords

Large Language Models, Instruction Tuning, Protein

## ACM Reference Format:

Wei Wu, Chao Wang, Liyi Chen, Mingze Yin, Yiheng Zhu, Kun Fu, Jieping Ye, Hui Xiong, and Zheng Wang. 2025. Structure-Enhanced Protein Instruction Tuning: Towards General-Purpose Protein Understanding with LLMs. In *Proceedings of the 31st ACM SIGKDD Conference on Knowledge Discovery and Data Mining V.2 (KDD '25), August 3–7, 2025, Toronto, ON, Canada*. ACM, New York, NY, USA, 21 pages. <https://doi.org/10.1145/3711896.3737138>

## Abstract

Proteins, as essential biomolecules, play a central role in biological processes, including metabolic reactions and DNA replication. Accurate prediction of their properties and functions is crucial in biological applications. Recent development of protein language models (pLMs) with supervised fine tuning provides a promising solution to this problem. However, the fine-tuned model is tailored for particular downstream prediction task, and achieving general-purpose protein understanding remains a challenge. In this paper, we introduce Structure-Enhanced Protein Instruction Tuning (SEPIT) framework to bridge this gap. Our approach incorporates a novel structure-aware module into pLMs to enrich their structural knowledge, and subsequently integrates these enhanced pLMs with large language models (LLMs) to advance protein understanding. In this framework, we propose a novel instruction tuning pipeline.

<sup>\*</sup>Corresponding author.

<sup>†</sup>Work done during the internship at Alibaba Cloud Computing.

Permission to make digital or hard copies of all or part of this work for personal or classroom use is granted without fee provided that copies are not made or distributed for profit or commercial advantage and that copies bear this notice and the full citation on the first page. Copyrights for components of this work owned by others than the author(s) must be honored. Abstracting with credit is permitted. To copy otherwise, or republish, to post on servers or to redistribute to lists, requires prior specific permission and/or a fee. Request permissions from [permissions@acm.org](mailto:permissions@acm.org).

KDD '25, Toronto, ON, Canada.

© 2025 Copyright held by the owner/author(s). Publication rights licensed to ACM.

ACM ISBN 979-8-4007-1454-2/25/08  
<https://doi.org/10.1145/3711896.3737138>

**KDD Availability Link:**

The code, datasets and model checkpoints of this paper has been made publicly available at <https://doi.org/10.5281/zenodo.15510090>.

## 1 Introduction

Proteins are large biomolecules and macromolecules composed of one or more long chains of amino acid residues. They play pivotal roles in catalyzing metabolic reactions, facilitating DNA replication, and driving other essential biological processes [5, 30]. Generally, proteins are represented in two types of forms: a *one-dimensional (1D) sequence*, which specifies the order of amino acids, and a *three-dimensional (3D) structure* which depicts the spatial configuration of the protein. A protein’s 1D sequence is generated by transcribing and translating a gene’s DNA sequence and subsequently folds into a specific 3D structure. This 3D conformation determines the protein’s properties and functions [64]. Conventional machine learning methods [67, 91] have achieved notable accuracy in protein property and function prediction via supervised learning. However, these methods are all task-specific as each model is restricted to predicting a particular property. The growing demand for comprehensive protein analysis in fields such as pathology and drug discovery [29] highlights the need for general-purpose protein understanding models capable of accurately predicting a wide range of protein properties and functions.

In the fast-evolving era of large language models (LLMs) [72, 93, 110], significant efforts have been made to leverage their semantic understanding and complex reasoning capabilities to achieve general-purpose protein property and function prediction. Initially, some approaches treat the 1D protein sequence as natural language input to LLMs [22, 59, 63, 81, 90]. However, they focus on learning associations between protein sequences and their properties or functions using only a limited subset of real-world protein sequences, which hinders the LLMs from generating reliable predictions at an evolutionary scale. To address this limitation, ProtST [98] and ProteinCLAP [55] utilize pLMs pre-trained on evolutionary-scale protein databases as protein sequence encoders and further employ contrastive learning [65] on protein-text paired data to incorporate functional information from text with high-quality protein representations from pLMs. Unfortunately, these methods remain restricted to prediction and retrieval tasks. However, real-world proteins exhibit complex and diverse properties and functions that require a more comprehensive understanding in an open-ended generative manner rather than being confined to specific tasks. To bridge this gap, Prot2Text [1], ProteinChat [29] and ProtT3 [56] propose protein-to-language generation by integrating protein sequence or structure encoding from pre-trained models.

Despite these advancements, existing methods still face significant challenges in providing reliable general-purpose protein understanding for scientific research applications. Firstly, although some studies acknowledge the critical role of a protein’s 3D structure in determining its properties and functions, proteins with directly available 3D structural information are rare. As a result, models must learn the relationship between 1D sequences and functional information while relying on limited 3D data, making it difficult to generate accurate property and function predictions. Secondly, existing protein-related instruction datasets overlook 3D structural information and provide limited coverage of protein properties and

functions. This gap hinders the comprehensive evaluation of model reliability and generalizability in general-purpose protein understanding tasks. Lastly, the vast diversity of protein properties and functions presents a major challenge for accurate prediction. Using a single general-purpose model to predict a wide range of complex properties and functions is more challenging than fine-tuning multiple specialized models for specific tasks.

To address these challenges, we propose a novel instruction tuning framework called Structure-Enhanced Protein Instruction Tuning (SEPIT) for general-purpose protein understanding. In this framework, we first design a structure-aware module within pLMs to obtain a protein sequence/structure-fused encoder, enabling support for different types of protein inputs (1D or 1D&3D). Following this, we implement a three-stage training pipeline. In stage 0 (warm-up stage), we train the protein sequence/structure-fused encoder using protein-text contrastive learning and structure denoising, allowing it to leverage a limited amount of structural information to enhance the understanding of large-scale sequence-only proteins. Then, we perform protein instruction tuning to equip LLMs for general-purpose protein understanding capability: in stage 1, we instill fundamental understanding of proteins into the model through protein caption instructions; in stage 2, we initialize mixture of experts (MoEs) through upcycling [42], which allows the model to learn more complex and diverse protein properties and functions while building upon the foundational knowledge from stage 1, all without increasing the number of activated parameters. To comprehensively evaluate the reliability and generalizability of our proposed framework, we construct the largest protein instruction dataset to date, which covers the most diverse range of protein properties and functions, based on large-scale protein knowledge bases [8, 84]. In summary, our key contributions are as follows:

- We designed and integrated a structure-aware module into protein language models, enabling the models to process various types of protein inputs. This significantly improved embedding quality compared to vanilla sequence-only pLMs.
- We constructed the largest and most extensive protein instruction dataset to date, addressing the gap in datasets for general-purpose protein understanding.
- We developed a novel protein instruction tuning strategy that allows a single model to learn a broad and complex range of protein properties and functions. This was achieved by leveraging MoEs built upon foundational knowledge.
- Using the proposed SEPIT framework and our curated protein instruction dataset, we demonstrated the feasibility of equipping large language models with general-purpose protein understanding capability.

## 2 Related Work

In this section, we present the key related work pertinent to our study, focusing primarily on protein language models. Additional related topics including multimodal instruction tuning and learning with 3D structural information are discussed in Appendix A.

Using context-aware language models [72], protein sequences can be treated like sentences, with amino acids acting as individual words. Through pre-training on databases containing hundreds of millions of such protein sequences (e.g., UniRef [80], BFD [75, 76]),

pLMs enable effective modeling and prediction of protein structures and functions [36]. In earlier works [4, 32, 77], LSTM and its variants [34, 37, 43, 102] were utilized to model the dependencies between residues in single protein sequences. With the rise of the Transformers architecture [85], Transformers-based pLMs emerged. ESM-1b [71], leveraging the Transformers architecture along with a masking strategy for pretraining, significantly enhances the prediction accuracy for mutational effects, secondary structure, and long-range contacts. After this, ProtTrans [20] released two auto-regressive models [16, 99] and four auto-encoder models [14, 18, 44, 68] pre-trained on protein sequence databases. Beyond merely focusing on single protein sequences, MSA Transformer [69] integrates multiple sequence alignments (MSA) of homologous proteins, providing a solid foundation for the success of AlphaFold2 [40] and AlphaFold3 [2]. Moreover, ESM-2 [53] further scaled up pLMs, achieving protein structure prediction performance comparable to previous works without utilizing MSA information, and significantly reduced inference overhead [52]. Additionally, there were other studies that attempted to incorporate additional knowledge into the pre-training of protein sequences. For example, ProteinBERT [11] and OntoProtein [104] incorporate Gene Ontology (GO) annotations directly into their protein embeddings. More recent methods—such as SaProt [78] and ESM-3 [31]—go further by fusing both sequence- and structure-based representations, thereby deepening the models’ grasp of protein characteristics. Although these protein language models produce rich, high-quality embeddings, they remain incapable of generating natural-language predictions about protein properties and functions.

### 3 Construction of Protein Instruction Dataset

To endow LLMs with general-purpose protein understanding capabilities and evaluate their reliability and generalizability, in this paper, we construct a protein instruction dataset contains open-ended generation and closed-set answer tasks. For the open-ended generation subset, we mainly constructed it based on Swiss-Prot [8]. We include almost all protein properties and functions contained therein (Function, Similarity, Subcellular location, Induction, Molecular Function, Biological Process, Cellular Component, Developmental Stage, Short Sequence Motif, Tissue Specificity, Activity Regulation, Pathway), and utilized ChatGPT [61] to aid in designing question templates based on the structured annotations. For the closed-set answer subset, we constructed it mainly based on the RCSB PDB [10]. We follow the data organized by previous researchers [29] and select parts of their proposed Q&A samples that are highly related to protein properties and functions, filtering out other samples related to metadata (e.g. discovery time and discovery methods). We have also sampled some examples related to Enzyme Commission (EC) and Gene Ontology (GO) predictions [26] for inclusion in the closed-set answer subset. More detailed information about the dataset, including statistical information and examples, is shown in Appendix B.

Compared to previously proposed protein-text datasets [22, 29, 90, 98], our dataset offers several key advantages: First, our dataset contains the most comprehensive set of instructions, covering nearly all critical protein properties and function types found in databases [8]. Second, with over 10 million instructions, along with

an additional 5 million supplementary instructions from TrEMBL, our dataset is the largest of its kind. Third, by incorporating structural data, our dataset enhances prediction reliability and provides a more robust foundation for protein understanding. In summary, our dataset serves as a valuable resource for advancing research in general-purpose protein understanding.

## 4 Structure-Enhanced Instruction Tuning

In this section, we provide a detailed introduction to our proposed SEPIT framework from two perspectives: model architecture and training pipeline.

### 4.1 Model Architecture

In this subsection, we introduce three main components of the SEPIT framework: 1) a sequence/structure fused protein encoder, 2) a linear projector, and 3) a large language model with MoEs modules. The model architecture is shown in Figure 1.

**Sequence/Structure Fused Protein Encoder.** Given the vast availability of sequence-only data and limited sequence-structure paired data (from both experimental and computational sources) within protein domain [75, 76, 80, 84], we propose a sequence/structure fused protein encoder that is capable of accommodating inputs in either form. Additionally, through leveraging the scarce sequence-structure paired data, we aim to enhance the model’s performance when dealing with sequence-only inputs.

For sequence-only data, numerous pLMs [11, 20, 53, 69, 71] have already been pre-trained on it. To facilitate their perception of structural information, we have designed a structure-aware module for pLMs. This module encodes the 3D structural information into the attention matrix and positional encoding of pLMs in a simple but effective way. Specifically, the attention mechanism of pLMs is defined as follows (for simplicity, we discuss the scenario with single-head and assume that the dimensions of the query, key, and value are all equal to the hidden size  $d$ ). Let  $\mathbf{X}^{(l)} = [\mathbf{x}_1^{(l)}, \mathbf{x}_2^{(l)}, \dots, \mathbf{x}_N^{(l)}]^\top$  denote the input to self-attention module in  $l$ -th layer, where  $\mathbf{x}_i^{(l)} \in \mathbb{R}^d$  is the  $d$ -dimension representation of the  $i$ -th residue out of the  $N$  residues in the protein. The self-attention module then works as follows:

$$\mathbf{A}^{(l)} = \frac{\mathbf{X}^{(l)} \mathbf{W}_Q^{(l)} (\mathbf{X}^{(l)} \mathbf{W}_K^{(l)})^\top}{\sqrt{d}}, \quad (1)$$

$$\text{Attn}(\mathbf{X}^{(l)}) = \text{softmax}(\mathbf{A}^{(l)}) \mathbf{X}^{(l)} \mathbf{W}_V^{(l)}, \quad (2)$$

where  $\mathbf{W}_Q^{(l)} \in \mathbb{R}^{d \times d}$ ,  $\mathbf{W}_K^{(l)} \in \mathbb{R}^{d \times d}$ ,  $\mathbf{W}_V^{(l)} \in \mathbb{R}^{d \times d}$ ,  $\mathbf{A}^{(l)}$  is the attention matrix,  $\mathbf{A}_{i,j}^{(l)}$  denotes the similarity between residue  $i$  and  $j$ . Inspired by previous work on geometric Transformers [58, 111], our structure-aware module takes the 3D coordinates  $\mathbf{C} = [\mathbf{c}_1, \mathbf{c}_2, \dots, \mathbf{c}_N]^\top$ ,  $\mathbf{c} \in \mathbb{R}^3$  of residues (alpha carbon atoms) as input and outputs the 3D feature matrix  $\Delta \in \mathbb{R}^{N \times N}$ , representing the pairwise spatial relationships of residues in 3D space:

$$\Delta = \phi(\psi_{(i,j)} \mathbf{W}_a) \mathbf{W}_b, \quad (3)$$

where  $\mathbf{W}_a \in \mathbb{R}^{K \times K}$ ,  $\mathbf{W}_b \in \mathbb{R}^{K \times 1}$  are linear transformation and  $\psi_{(i,j)} = [\psi_{(i,j)}^1, \dots, \psi_{(i,j)}^K]^\top$  is the Euclidean distance for each twosome of residues undergoes a transformation via the Gaussian

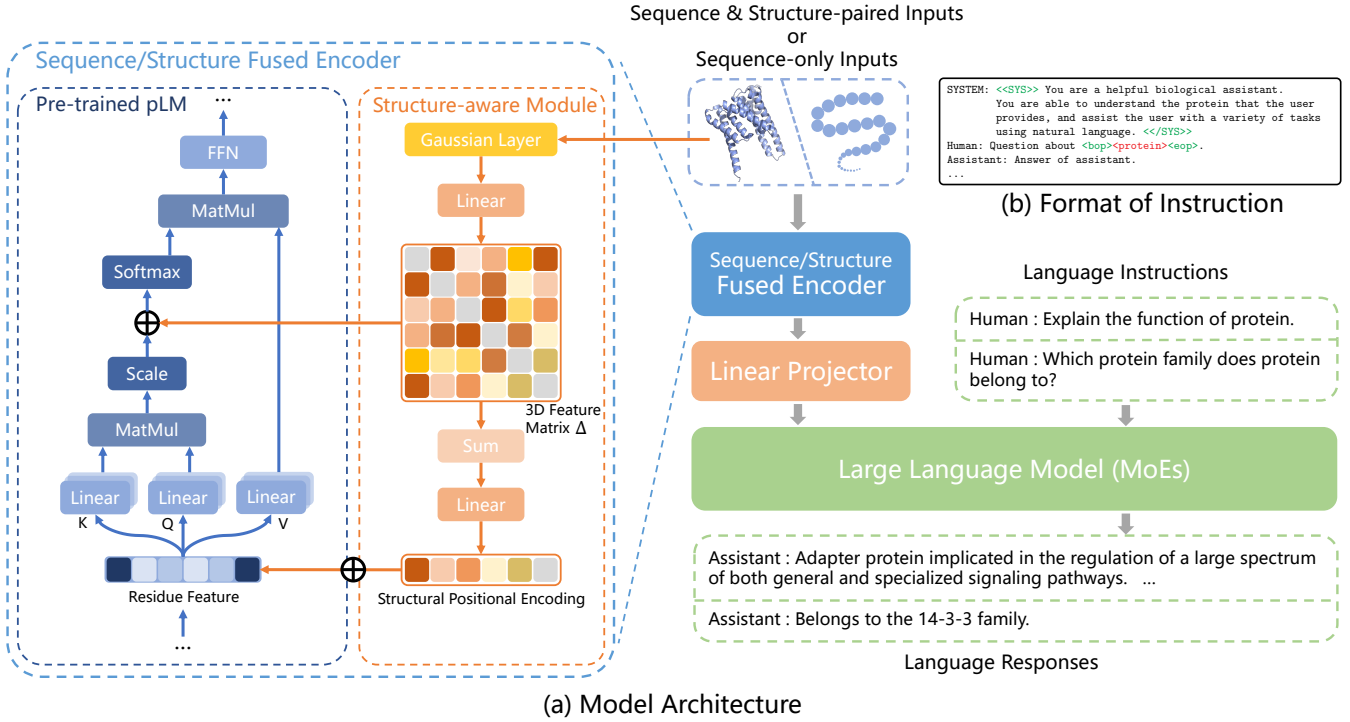


**Figure 1: (a) The model architecture of the SEPIT framework includes sequence/structure fused protein encoder, linear projector, and LLMs with MoEs modules, (b) example of instruction format.**

Basis Kernel function [73]:

$$\psi_{(i,j)}^k = -\frac{1}{\sqrt{2\pi}|\sigma^k|} \exp\left(-\frac{1}{2} \left( \frac{\|c_i - c_j\| - \mu^k}{|\sigma^k|} \right)^2\right), \quad k = 1, \dots, K, \quad (4)$$

where the learnable parameters  $\mu^k$  and  $\sigma^k$  correspond to the center and scaling coefficient of the  $k$ -th Gaussian Basis Kernel. These relationships are incorporated into the attention matrix as bias:

$$\hat{A}^{(l)} = A^{(l)} + \Delta, \quad (5)$$

and added as structure positional encoding to the input of pLMs:

$$\hat{X}^{(0)} = X^{(0)} + \omega \left( \sum_{j \in [n]} \psi_{(i,j)} \right) W_c, \quad (6)$$

where  $\omega$  signifies the coefficient that regulates the magnitude of the structure positional encoding and  $W_c \in \mathbb{R}^{K \times d}$  is learnable linear transformation. It is noteworthy that when the input to the sequence/structure fused protein encoder consists solely of the protein sequence, lacking structural information, the structure-aware module will be automatically disabled. This allows it to adapt to different protein input formats.

**Linear Projector.** To bridge proteins with natural language, a module is required to link the protein encoder and the LLMs decoder. Prior work in the MLLMs field has contributed outstanding methods such as Q-former [46], linear projector [54], and merging tokens before the linear projector [112]. Considering the vast differences between proteins and visual images - that is, the former requires the retention of more information of all residues (as any change in the amino acid sequence can lead to significant structural differences,

resulting in profoundly different properties and functions), whereas the latter possesses some degree of information redundancy - we opt for a simple linear projector to reduce information loss.

**Large Language Model with Mixture of Experts Module.** Due to the understanding of proteins being a complex multi-task problem, the various properties and functions of proteins can exhibit significant changes with subtle variations in the amino acid sequence. As the hub of "understanding" within the entire framework, the capabilities of LLMs are crucial. Previous scaling laws [41] have suggested that larger parameter sizes can endow LLMs with stronger capabilities; however, the additional computation costs brought about by increased activated parameters are intolerable for us. Therefore, we seek to leverage mixture-of-experts (MoEs) to achieve higher parameter sizes without increasing the number of activated parameters, thereby enhancing the model's capacity and generalization ability. In our framework, the MoEs module replaces the FFN module in each Transformer decoder layer. The MoEs module works as follows [38, 45, 50, 97, 106, 113]:

$$y = \sum_{i=1}^{n_e} G(\mathbf{x})_i \cdot E_i(\mathbf{x}). \quad (7)$$

Here,  $\mathbf{x}$  is assumed to be the input to the original FFN layer, and  $E$  represents the  $n_e$  experts in the MoEs, each of which has the exact same structure as the original FFN layer.  $G$  represents the gating network,  $G(\mathbf{x})_i$  denotes the gate weight for the  $i$ -th expert, and  $E_i(\mathbf{x})$  is the output of the  $i$ -th expert. For the gating network, we employ the commonly used linear TopK gate:

$$G(\mathbf{x}) := \text{Softmax}(\text{TopK}(\mathbf{x} \cdot \mathbf{W}_G)), \quad (8)$$

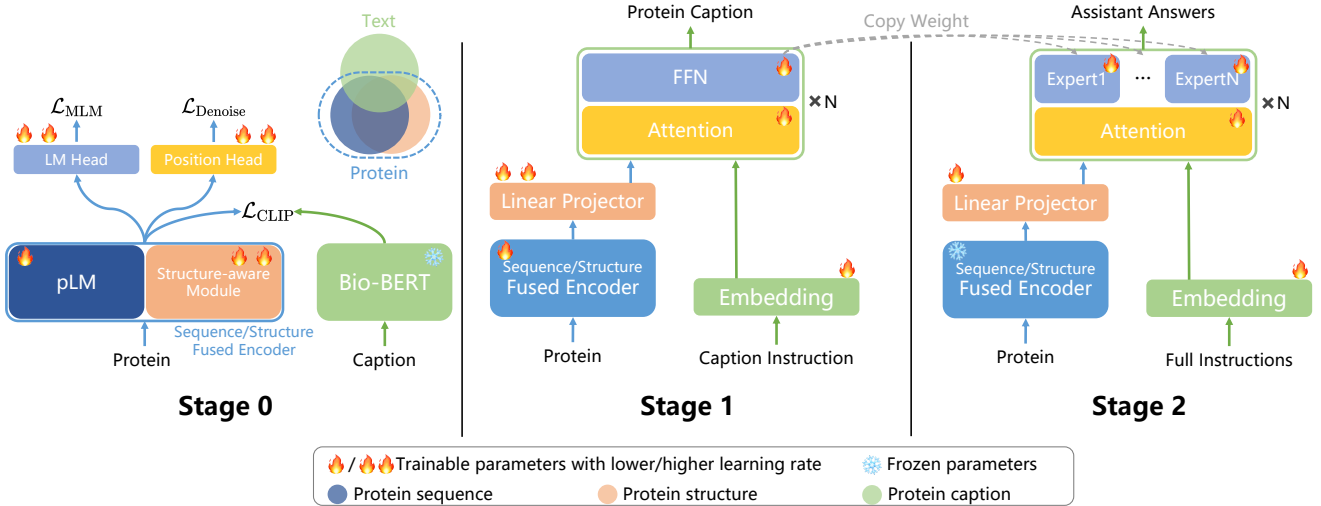


**Figure 2: The three-stage training pipeline of SEPIT with a warm-up stage (stage 0) for protein encoder and two instruction tuning stages (stage 1 & stage 2).**

and we impose auxiliary loss to ensure the token balance among the experts [45, 113]:

$$\mathcal{L}_{\text{aux}} = n \cdot \sum_{i=1}^n f_i \cdot p_i, \quad (9)$$

where  $f_i$  is the proportion of tokens processed by expert  $i$  and  $p_i$  represents the proportion of gating weight allocated to an expert.

## 4.2 Training Pipeline

In this subsection, we will discuss the details of the training pipeline for SEPIT framework, based on the model architecture presented before. As shown in Figure 2, the whole pipeline includes three stages: in stage 0, we warm up our proposed sequence/structure fused protein encoder based on pre-trained pLM primarily through protein-text contrastive learning and structure denoising. In stage 1, we pre-train on the protein captioning task to further align protein representations with natural language, while concurrently infusing foundational protein knowledge into LLMs. In stage 2, we initiate the MoEs modules using the sparse upcycling [42] from the FFNs of the LLMs trained in stage 1 and perform instruction tuning on our proposed protein instruction dataset.

### Stage 0: Warming Up the Sequence/Structure Fused Protein Encoder.

In this stage, our primary goal is to warm up our protein encoder. Although the pLM is already pre-trained, the structure-aware module that we plug in is randomly initialized. To address this, we leverage two main pre-training paradigms. Firstly, to enable the structure-aware module to better perceive structural information, we follow the common practice in molecular self-supervised learning [27, 58, 103, 111], which involves structure denoising tasks. For the input 3D coordinates of protein residues  $C = [c_1, c_2, \dots, c_N]^\top$ , we apply noise to obtain noised coordinates  $\tilde{C} = [\tilde{c}_1, \tilde{c}_2, \dots, \tilde{c}_N]^\top$ , where  $\tilde{c}_i = c_i + \alpha \delta_i$ ,  $\delta_i \sim \mathcal{N}(0, I)$ ,  $\alpha$  is a scalar used to control the magnitude of noise. Then we predict the applied noise based on them (equivalent to predicting the original

3D coordinates). The formula for denoise loss is as follows:

$$\mathcal{L}_{\text{Denoise}} = \frac{1}{3n} \sum_{i=1}^n \sum_{j=1}^3 (\delta_i^j - \hat{\delta}_i^j)^2, \quad (10)$$

where  $\hat{\delta}_i^j$  is output by an additional SE(3) equivariant attention layer [58, 74] (position head), which takes the last hidden state of the protein encoder  $X^{(L+1)}$  and  $\Delta$  in Equation 5 as input:

$$\hat{\delta}_i^j = \left( \sum_{i=1}^n \Delta_{ik} D_{ik}^j X_k^{(L+1)} W_m \right) W_n, \quad D_{ik} = \frac{c_i - c_k}{\|c_i - c_k\|}. \quad (11)$$

Secondly, we utilize protein-text contrastive learning to further promote the fusion of protein sequence and structure information under text supervision, while concurrently aligning protein representations with their textual descriptions. Formally, given a batch of paired proteins and protein captions  $\{(\mathcal{P}_i, \mathcal{T}_i)\}_{i=1}^B$ , the CLIP loss can be expressed as:

$$\mathcal{L}_{\text{CLIP}} = -\frac{1}{2B} \sum_{i=1}^B \left( \log \frac{\exp(\mathbf{p}_i \cdot \mathbf{t}_i / \tau)}{\sum_{j=1}^B \exp(\mathbf{p}_i \cdot \mathbf{t}_j / \tau)} + \log \frac{\exp(\mathbf{p}_i \cdot \mathbf{t}_i / \tau)}{\sum_{j=1}^B \exp(\mathbf{p}_j \cdot \mathbf{t}_i / \tau)} \right), \quad (12)$$

where  $\mathbf{p}_i, \mathbf{t}_i$  are the representations of  $P_i$  and  $T_i$  output by the protein encoder and text encoder (BERT), respectively. Additionally, we also maintain the Masked Language Model (MLM) training objective related to the protein sequence (consistent with ESM2 [53]) as a regularization term to prevent catastrophic forgetting in the pLM. Overall, the loss for stage 0 is as follows:

$$\mathcal{L}_{\text{stage 0}} = \mathcal{L}_{\text{Denoise}} + \mathcal{L}_{\text{CLIP}} + \mathcal{L}_{\text{MLM}}. \quad (13)$$

Under the influence of these training objectives, the mutual information between protein sequence and protein structure as well as protein and text is increased.

**Stage 1: Pre-training on Protein Captions.** In this stage, our fundamental objective is to further align proteins with their natural language descriptions through the paradigm of conditional generation [54, 62], utilizing protein caption instructions. To ensure consistency in the model's handling of different forms of protein inputs, we randomly input protein data, both those with only sequences and those paired with structures, into our protein encoder

**Table 1: Performance comparisons on open-ended generation and closed-set answer tasks.**

Model	Activated Parameters	Open-Ended								Closed-Set Accuracy	
		BLEU-2	BLEU-4	ROUGE-1	ROUGE-2	ROUGE-L	METEOR	BERT-P	BERT-R		
<b>Zero-Shot</b>											
GPT-3.5-turbo	N/A	3.26	0.02	12.41	3.14	11.06	10.44	85.18	85.40	85.24	56.56%
Claude-3-haiku	N/A	3.00	0.07	12.10	2.65	10.62	9.28	86.04	85.47	85.70	59.14%
GPT-4-turbo	N/A	4.21	0.08	12.78	2.93	11.57	10.41	86.91	85.56	85.71	58.58%
GPT-4o-mini	N/A	2.36	0.01	10.72	1.93	9.03	9.00	85.08	85.38	85.19	41.58%
GPT-4o	N/A	3.26	0.14	15.02	3.73	12.30	13.01	85.28	86.51	85.86	59.70%
DeepSeek-V3	671B	2.75	0.02	12.15	3.37	10.54	10.25	85.32	85.63	85.44	56.49%
Galactica	1.3B	0.43	0.01	3.49	0.41	2.67	2.44	85.79	82.61	84.08	39.15%
BioMedGPT	7B	0.83	0.01	4.90	0.49	3.26	4.59	85.51	84.95	85.14	38.61%
Mol-Instructions	7B	0.53	0.01	5.96	0.39	4.64	5.51	83.81	84.41	84.06	—
BioT5+	252M	3.88	1.92	12.12	4.88	10.37	14.26	85.14	85.93	85.48	—
InstructProtein	1.3B	5.50	2.97	14.80	5.68	13.76	13.17	85.34	85.92	85.57	48.37%
<b>Instruction Tuning</b>											
TinyLlama	1.1B	51.16	43.44	65.41	51.26	62.31	60.80	93.97	94.37	94.16	74.09%
OpenLlama-v2	3B	36.19	30.65	48.33	36.52	45.53	49.01	92.92	91.87	92.35	71.77%
Llama2	7B	57.02	49.47	70.80	57.24	67.78	65.96	94.95	95.17	95.05	71.68%
<b>Sequence-Only Protein Instruction Tuning</b>											
PIT-TinyLlama	1.8B	57.82	50.02	71.34	58.16	68.35	66.19	95.18	95.28	95.26	76.02%
PIT-TinyLlama-MoEs	1.8B	57.92	50.01	72.13	58.21	69.19	66.29	95.31	95.30	95.29	78.56%
<b>Structure-Enhanced Protein Instruction Tuning</b>											
SEPI-TinyLlama	1.8B	58.43	51.04	72.34	58.77	69.13	67.91	95.32	95.59	95.44	79.05%
<b>SEPI-TinyLlama2</b>	<b>8B</b>	<b>60.81</b>	<b>52.37</b>	<b>74.80</b>	<b>60.84</b>	<b>71.62</b>	<b>68.43</b>	<b>95.81</b>	<b>95.73</b>	<b>95.76</b>	<b>79.97%</b>
<b>SEPI-TinyLlama-MoEs</b>	<b>1.8B</b>	<b>60.28</b>	<b>52.16</b>	<b>74.22</b>	<b>60.29</b>	<b>71.13</b>	<b>68.27</b>	<b>95.62</b>	<b>95.69</b>	<b>95.64</b>	<b>79.73%</b>

at probabilities of 15% and 85%, respectively. The output protein representation sequences are mapped into the textual space through linear projector, in conjunction with protein caption instructions to guide LLMs in producing straightforward descriptions of proteins, such as function, family, subcellular localization, and overall descriptions. Formally, consider a protein-text pair  $(\mathcal{P}, \mathcal{T})$  similar to that in stage 0, given the output sequence of the protein encoder  $S_p$ , and instructions  $S_{\text{instruct}}$ , the objective of stage 1 is as follows:

$$\mathcal{L}_{\text{stage 1}} = p(S_t | f(S_p), S_{\text{instruct}}) = \prod_{i=1}^L p_{\theta}(s_i | S_p, S_{\text{instruct}, < i}, S_{t, < i}), \quad (14)$$

where  $f(\cdot)$  denotes the linear projector,  $\theta$  represents all trainable parameters,  $S_{\text{instruct}, < i}$  and  $S_{t, < i}$  respectively signify the instruction and answer tokens preceding the current prediction token  $s_i$ , and  $L$  denotes the total sequence length accepted by LLMs.

**Stage 2: Upcycling and Instruction Tuning.** In this stage, our main aim is to upcycle the model obtained from stage 1 by replacing each FFN module within the LLMs with MoE module, where each expert is initialized by an FFN. In the case of top-1 activation, this approach offers a larger model parameter count under the same activation parameter volume. Meanwhile, the basic understanding of proteins acquired in stage 1 lays the groundwork for more complex and multifaceted learning in this stage. Based on this, we utilize a diverse set of protein instructions for instruction tuning, aiming to endow SEPI with general-purpose protein understanding capabilities. Similar to stage 1, the loss function for stage 2 can be formally represented as:

$$\mathcal{L}_{\text{stage 2}} = \mathcal{L}_{\text{stage 1}} + \beta \mathcal{L}_{\text{aux}}, \quad (15)$$

where  $\mathcal{L}_{\text{aux}}$  is an auxiliary loss used for constraining the token balance among experts, as mentioned in Equation 9, with  $\beta$  being used to control its relative magnitude.

## 5 Experiments

In this section, we will first outline the experimental setting. Subsequently, we will demonstrate SEPI’s effectiveness and design benefits via performance comparisons and ablation studies. Finally, we will delve deeper into the characteristics of SEPI through generalization analysis and case studies. Additional analysis, including error pattern analysis are provided in the Appendix C.5.

### 5.1 Experimental Setting

First, we provide a brief overview of the main experimental settings, with more detailed information available in Appendix B, C.1.

**Use of Pre-training Data.** In each stage of SEPI, we utilize our proposed protein instruction dataset, employing different subsets at various stages. At Stage 0, our focus is primarily on basic protein descriptions derived from Swiss-Prot and the RCSB PDB. For Swiss-Prot, akin to previous work [98], we formulate the protein captions using Function, Similarity and Subcellular location. Regarding the RCSB PDB, we directly utilize abstracts from related PubMed papers collected by [29] as captions. In Stage 1, we employ the same data as in Stage 0, but the output format is altered to the style of caption instructions. During Stage 2, we utilize the complete protein instruction dataset we proposed, which includes open-ended generation and closed-set answers tasks.

**Table 2: Performance comparisons on overlapping properties and functions.**

Model	Activated Parameters	Open-Ended								Closed-Set Accuracy	
		BLEU-2	BLEU-4	ROUGE-1	ROUGE-2	ROUGE-L	METEOR	BERT-P	BERT-R	BERT-F1	
ProtT3	1.3B	65.38	51.87	73.75	57.88	72.88	70.39	96.29	95.80	96.03	90.52%
<b>SEPI-TinyLlama-MoEs</b>	1.8B	<b>83.07</b>	<b>81.29</b>	<b>86.74</b>	<b>83.55</b>	<b>86.05</b>	<b>85.96</b>	<b>98.04</b>	<b>98.01</b>	<b>98.02</b>	<b>94.92%</b>

**Table 3: Ablation study on SEPI-T’s architecture.**

Model	Open-Ended			Closed-Set Accuracy
	BLEU-2	ROUGE-L	METEOR	
SEPI-TinyLlama-MoEs	<b>60.28</b>	<b>71.13</b>	<b>68.27</b>	<b>79.73%</b>
w/o Structure	↓ 4.08%	↓ 2.81%	↓ 2.98%	↓ 1.48%
w/o MoEs	↓ 3.17%	↓ 2.90%	↓ 0.52%	↓ 0.86%
w/o Structure & MoEs	↓ 4.26%	↓ 4.07%	↓ 3.13%	↓ 4.88%
w/o Stage 0	—	—	—	—
w/o SEPI-T	↓ 17.83%	↓ 14.17%	↓ 12.28%	↓ 7.61%
w/ TrEMBL	↓ 2.69%	↓ 2.13%	↓ 2.00%	↓ 0.26%

**Baselines and Evaluation Metrics.** We evaluate the capability of SEPI-T for general-purpose protein understanding on the test set of the protein instruction dataset we proposed with the state-of-the-art models. There are four main categories of methods. Among the Zero-Shot methods, we include current mainstream LLMs providing API services (e.g., Claude-3-haiku [6], GPT-3.5-turbo/4-turbo/40-mini/40 [61] and DeepSeek-V3 [17]), open-source LLMs fine-tuned on biomedical corpus (e.g., Galactica [81], BioMedGPT [59]) and open-source LLMs fine-tuned specifically on molecular or protein knowledge (e.g., Mol-Instructions [22], BioT5+ [63], InstructProtein [90] and ProtT3 [56]). In the category of instruction tuning methods, we evaluate mainstream open-source LLMs (e.g., TinyLlama-Chat [105], OpenLlama-v2 [25], Llama2-Chat [83]), where the protein sequences are input in natural language form. For sequence-only protein instruction tuning methods (PITs), ESM2-650M [53] was utilized as the protein encoder, with only protein sequences input. In addition to our proposed SEPI-T framework, SEPI-TinyLlama-MoEs, we have also designed two variants that differ in the LLMs’ architecture. For evaluation metrics, we employ BLEU score [79], ROUGE score [51], METEOR score [9], BERT score [107] calculated by PubMedBERT [28], and Accuracy to assess performance across two types of tasks: open-ended generation and closed-set answer, respectively.

## 5.2 Performance Comparisons

The results of performance comparisons are shown in Table 1. We can observe that: 1) Our proposed SEPI-T consistently outperforms the baseline models by a significant margin. Specifically, SEPI-T-Llama achieves the highest performance across all metrics in both types of tasks. In comparison, SEPI-TinyLlama-MoEs demonstrates significantly higher parameter efficiency, achieving almost identical results to SEPI-T-Llama with just 1/6 of the LLMs’ activated parameters. 2) Zero-Shot methods generally perform poorly, with neither powerful general models like GPT and Claude nor open-source models fine-tuned on biomedical corpus or protein knowledge able to accomplish protein understanding tasks well. Notably,

**Table 4: Performance of SEPI-T’s encoder.**

Model	EC	GO		
		BP	MF	CC
ProtBert [11]	0.838	0.279	0.456	0.408
OntoProtein [104]	0.841	0.436	0.631	0.441
ESM1b [71]	0.869	0.452	0.659	0.477
ESM2 [53]	0.874	0.472	0.662	0.472
CDConv [21]	0.820	0.453	0.654	0.479
GearNet [109]	0.810	0.400	0.581	0.430
ProtST-ESM2 [98]	0.878	<b>0.482</b>	0.668	0.487
<b>SEPI-T’s Encoder</b>	<b>0.893</b>	0.476	<b>0.674</b>	<b>0.497</b>

Mol-Instructions and BioT5+ are trained on protein-related instructions. However, limited data diversity causes catastrophic forgetting to instruction following, hindering their ability to provide closed-set answers or accurate open-ended responses. 3) Instruction tuning on pure LLMs endows LLMs with decent protein understanding capabilities and demonstrates certain scaling laws [41] (OpenLlama-v2 demonstrates suboptimal results as it has not been specifically fine-tuned for chat assistant purpose.) However, overall, due to the lack of prior knowledge learned from evolutionary-scale protein databases, they can only achieve limited performance. 4) While utilizing prior knowledge from pLMs can significantly enhance the performance of LLMs of the same scale, the lack of structural awareness in PIT only results in suboptimal outcomes compared to our proposed SEPI-T.

Considering that there are additional related works [29, 56, 60] capable of captioning input protein sequences but lacking instruction-following capabilities, we attempted to compare performance on overlapping properties and functions with these works. Table 2 shows a performance comparison with ProtT3 [56], which is the most representative among these works, demonstrates superior performance. For open-ended generation and closed-set answer tasks, we specifically selected Function, Similarity, Subcellular location, and overlapping Q&A about proteins from RCSB PDB for comparison. The results demonstrate that our model exhibits significantly better performance.

## 5.3 Ablation Studies

In this section, we will explore the impact of various designs of SEPI-T on its performance from two aspects: the model and the data.

**Model Ablation.** For SEPI-T’s model architecture, we propose the following variants: without the structure-aware module (w/o Structure), without the mixture of experts module (w/o MoEs), without both the aforementioned modules (w/o Structure & MoEs), without Stage 0 pre-training (w/o Stage 0), and completely excluding the SEPI-T framework (w/o SEPI-T). Table 3 shows the results

**Table 5: Performance comparisons with different protein input formats (all models are based on TinyLlama).**

Model	PIT	PIT -MoEs	SEPIT	SEPIT -MoEs	SEPIT -MoEs	SEPIT -MoEs
<b>Input Formation</b>						
Train w/ Struct.	✗	✗	✓	✓	✓	✓
Infer w/ Struct.	✗	✗	✓	✗	✓	✗
<b>Open-Ended</b>						
BLEU-2	57.82	57.92	58.43	57.95	60.28	59.98
ROUGE-L	68.35	69.19	69.13	68.75	71.13	70.87
METEOR	66.19	66.29	67.91	67.54	68.27	68.00
BERT-F1	95.26	95.29	95.44	95.38	95.64	95.59
<b>Closed-Set</b>						
Accuracy	76.02%	78.56%	79.05%	77.80%	79.73%	79.53%

of the ablation study, proving the significant effectiveness of each component within SEPIT’s model architecture. The absence of either the structure-aware module or the MoEs Module leads to performance degradation in both open-ended generation tasks and closed-set answer tasks, with further deterioration when both are excluded. Meanwhile, the performance under w/o SEPIT intuitively demonstrates the overall effectiveness of the framework. It is noteworthy that the results for w/o Stage 0 are not available, as under the implementation using automatic mixed precision (AMP) based on FP16, the randomly initialized structure-aware module would bring excessively large gradients causing overflow, even though we employed a warm-up learning rate scheduler. Due to device restrictions, we were unable to use BF16 type; however, this issue was resolved as Stage 0 progressed. In order to supplement the analysis of the effectiveness of Stage 0, we validate the protein encoder trained by Stage 0 on commonly used EC, GO annotation tasks [26]. The results, as shown in Table 4, demonstrate the performance comparisons to state-of-the-art methods on  $F_{max}$  metric.

**Data Ablation.** Regarding the data, apart from using Swiss-Prot and RCSB PDB for constructing the protein instruction dataset, there exists a substantial amount of protein-text paired data in TrEMBL [8]. Considering that the TrEMBL data is annotated by automated methods and has not been manually screened, we select proteins with more comprehensive descriptions (annotation score  $\geq 4$ ) to construct a supplementary dataset using the same method, with a sample size (5.25M) close to the entire protein instruction dataset (5.47M). Disappointingly, as shown in Table 3 (w/ TrEMBL), even after doubling the GPUs cost, what we obtain is a decrease in performance. Our analysis suggests that directly mixing low-quality data into high-quality data introduces noise, and protein understanding tasks require higher quality over quantity for data. More results can be found in Appendix C.3.

#### 5.4 Generalization Analysis

**Generalization Across Different Protein Input Formats.** Towards a general-purpose protein understanding capability, SEPIT supports both sequence-only and sequence-structure paired protein inputs, achieving consistent results as shown in Table 5. The three SEPIT variants all yields very similar effects on both types of protein

**Table 6: Performance comparisons on OOD proteins.**

Model	BLEU-2	ROUGE-L	METEOR	BERT-F1
TinyLlama	22.23	35.39	35.27	90.26
Llama2	28.51	41.63	41.58	91.27
PIT-TinyLlama	37.59	50.60	48.61	92.73
PIT-TinyLlama-MoEs	38.37	50.09	51.10	92.70
SEPIT-TinyLlama	40.25	52.03	52.18	93.02
+ w/o input structure	39.75	51.84	52.24	93.00
SEPIT-TinyLlama-MoEs	41.60	54.26	51.91	93.30
+ w/o input structure	41.26	53.85	51.52	93.23

inputs. Moreover, compared to the corresponding scale PIT model, SEPIT demonstrates a stronger understanding of sequence-only inputs. This implies that through SEPIT, we can utilize a small amount of sequence-structure paired data to enhance the understanding of a large volume of sequence-only protein inputs.

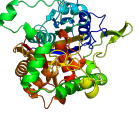
**Generalization to Out-of-Distribution Proteins.** To further evaluate the generalization ability of SEPIT on highly novel proteins, we constructed an out-of-distribution (OOD) test dataset by filtering sequences with a maximum amino acid similarity of  $< 40\%$  using the CD-HIT clustering algorithm [23]. As shown in Table 6, all methods exhibited performance drops on this challenging setup, with instruction tuning methods being particularly affected. However, SEPIT demonstrated stronger generalization compared to alternative approaches, owing to its integration of both PLMs’ prior knowledge and the structural information. Remarkably, SEPIT maintained its performance even without structural input during inference, highlighting its robust generalization capacity.

#### 5.5 Case Studies

**General-Purpose Protein Understanding Ability of SEPIT.** At last, we would like to showcase the general-purpose protein understanding capability of SEPIT. As shown in Table 7, we present three cases from the test set of our protein instruction dataset. For case 1, SEPIT accurately responds regarding the protein’s function, whereas PIT incorporates incorrect details, and both Llama-Chat and GPT-4 offer entirely inaccurate responses. For case 2, SEPIT also gives the correct response, while the answers from PIT and Llama-Chat, although covering the correct answer, come with additional incorrect information, likely due to hallucinations caused by the lack of structural information. For case 3, SEPIT provides the partially correct response, whereas PIT and Llama-Chat exhibit a similar error pattern to case 2. Due to space limitations, more cases and analysis are included in the Appendix C.4, C.5.

**Workload of Experts in SEPIT.** In SEPIT, we utilize mixture of experts, and in Figure 3, we present the workload distribution of different experts during inference on test set of the open-ended generation task. In the left graph, we can observe that the experts are evenly activated, indicating that the auxiliary loss has played its expected role, which lays the foundation for efficient parallel inference of experts. In the right graph, we visualize the pathways distribution of text and protein tokens across experts in different layers, and we observe an intriguing phenomenon. Unlike the

**Table 7: Case studies on general-purpose protein understanding ability of SEPIT.**

 P9WF36 (Swiss-Prot)	<b>Question:</b> Explain the function of <protein>. <b>Ground Truth:</b> Acts as a transcriptional regulator. Probably redox-responsive. The apo- but not holo-form probably binds DNA (By similarity). <b>SEPIT-TinyLlama-MoEs:</b> Acts as a transcriptional regulator. Probably redox-responsive. The apo- but not holo-form probably binds DNA. <b>PIT-TinyLlama-MoEs:</b> Acts as a transcriptional regulator, probably involved in antibiotic resistance gene expression. Binds DNA (By similarity). <b>Llama-Chat:</b> Involved in resistance toward heavy metals (PubMed:12839546). Binds cadmium or lead ions but not zinc ions (By similarity). <b>May be involved in intracellular transport of Cd(+) or Pb(+) as well as their detoxification by sequestration into vacuoles (Probable) (PubMed:17081065).</b> <b>GPT-4-turbo:</b> The string you've provided appears to be an amino acid sequence of a protein. However, without additional context or data, I cannot provide a function caption for this specific sequence directly.
	<b>Question:</b> Which GO terms outline the biological processes of <protein>? <b>Ground Truth:</b> fatty acid beta-oxidation <b>SEPIT-TinyLlama-MoEs:</b> fatty acid beta-oxidation <b>PIT-TinyLlama-MoEs:</b> fatty acid beta-oxidation; phenylacetate catabolic process <b>Llama-Chat:</b> fatty acid beta-oxidation; phenylacetate catabolic process <b>GPT-4-turbo:</b> To understand the biological processes of the provided protein sequence, one must first consider its origin, functions, and structure. However, without direct access to databases or running bioinformatic tools right now...
 A0KR49 (Swiss-Prot)	<b>Question:</b> What is the protein family of <protein>? <b>Ground Truth:</b> Belongs to the metallo-dependent hydrolases superfamily. Atu3266/EF_0837 deacetylase family. <b>SEPIT-TinyLlama-MoEs:</b> Belongs to the metallo-dependent hydrolases superfamily. <b>PIT-TinyLlama-MoEs:</b> Belongs to the metallo-dependent hydrolases superfamily. Type II family. <b>Llama-Chat:</b> Belongs to the metallo-dependent hydrolases superfamily. Hut1 family. <b>GPT-4-turbo:</b> To understand the biological processes of the provided protein sequence, one must first consider its origin, functions, and structure. However, without direct access to databases or running bioinformatic tools right now...
 Q7CS13 (Swiss-Prot)	<b>Question:</b> What is the protein family of <protein>? <b>Ground Truth:</b> Belongs to the metallo-dependent hydrolases superfamily. Atu3266/EF_0837 deacetylase family. <b>SEPIT-TinyLlama-MoEs:</b> Belongs to the metallo-dependent hydrolases superfamily. <b>PIT-TinyLlama-MoEs:</b> Belongs to the metallo-dependent hydrolases superfamily. Type II family. <b>Llama-Chat:</b> Belongs to the metallo-dependent hydrolases superfamily. Hut1 family. <b>GPT-4-turbo:</b> To understand the biological processes of the provided protein sequence, one must first consider its origin, functions, and structure. However, without direct access to databases or running bioinformatic tools right now...

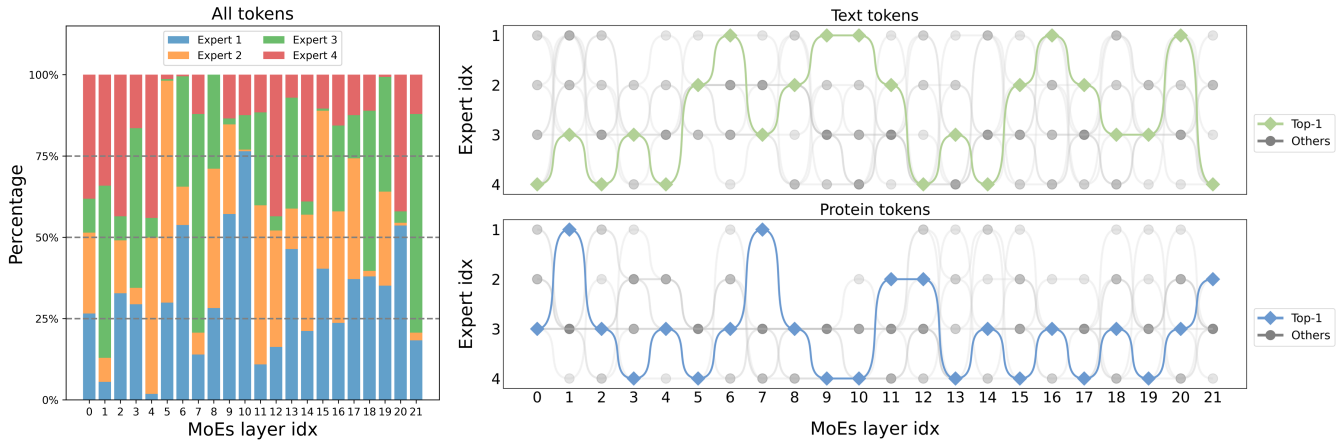


**Figure 3: The workload of experts in SEPIT (left) and tokens' pathways among experts (right).**

findings in previous vision-language multimodal research [50], in SEPIT, text and protein tokens are processed by different experts instead of following almost identical pathways as do text and image tokens. We believe that this stems from the fundamental difference between proteins and images. That is, protein tokens, which represent amino acids, cannot reflect the properties of the entire protein, while image tokens represent specific regions of an image containing independent information that can correspond to a part of the image’s caption. This validates our choice to use complete protein representation sequences as inputs for LLMs, rather than compressing tokens as is often done in vision-language tasks. More visualization is shown in Appendix C.4.

## 6 Conclusion

In this work, we introduce SEPIT, a novel approach for general-purpose protein understanding. SEPIT is designed to enable LLMs to interpret both the sequence and structural information of proteins, allowing them to follow instructions and generate precise

insights into protein properties and functions. To achieve this, we integrate structure-aware enhancements into pre-trained pLMs and connect them to LLMs via a linear projector. The models are then trained using a two-stage instruction tuning pipeline on the largest protein instruction dataset to date, which we constructed. Experimental results demonstrate that SEPIT significantly outperforms the state-of-the-art models, highlighting its effectiveness in advancing general-purpose protein understanding.

## Acknowledgment

This work was supported in part by the National Key R&D Program of China (Grant No.2023YFF0725001), in part by the National Natural Science Foundation of China (Grant No.92370204), in part by the Guangdong Basic and Applied Basic Research Foundation (Grant No.2023B1515120057), Education Bureau of Guangzhou Municipality.

## References

[1] Hadi Abdine, Michail Chatzianastasis, Costas Bouyioukos, and Michalis Vazirgiannis. 2024. Prot2text: Multimodal protein's function generation with GNNs and transformers. In Proc. of AAAI. 10757–10765.

[2] Josh Abramson, Jonas Adler, Jack Dunger, Richard Evans, Tim Green, Alexander Pritzel, Olaf Ronneberger, Lindsay Willmore, Andrew J Ballard, Joshua Bambrick, et al. 2024. Accurate structure prediction of biomolecular interactions with AlphaFold 3. *Nature* (2024), 1–3.

[3] Jean-Baptiste Alayrac, Jeff Donahue, Pauline Luc, Antoine Miech, Iain Barr, Yana Hasson, Karel Lenc, Arthur Mensch, Katherine Millican, Malcolm Reynolds, et al. 2022. Flamingo: a visual language model for few-shot learning. *Proc. of NeurIPS* (2022), 23716–23736.

[4] Ethan C Alley, Grigory Khimulya, Surojit Biswas, Mohammed AlQuraishi, and George M Church. 2019. Unified rational protein engineering with sequence-based deep representation learning. *Nature methods* (2019), 1315–1322.

[5] Christian B Anfinsen and Edgar Haber. 1961. Studies on the reduction and re-formation of protein disulfide bonds. *Journal of Biological Chemistry* (1961), 1361–1363.

[6] Anthropic. 2024. Claude 3 Haiku: our fastest model yet. <https://www.anthropic.com/news/clause-3-haiku>

[7] Jinze Bai, Shuai Bai, Shusheng Yang, Shijie Wang, Sinan Tan, Peng Wang, Junyang Lin, Chang Zhou, and Jingren Zhou. 2023. Qwen-VL: A Versatile Vision-Language Model for Understanding, Localization, Text Reading, and Beyond. *arXiv:2308.12966 [cs.CV]* <https://arxiv.org/abs/2308.12966>

[8] Amos Bairoch and Rolf Apweiler. 1997. The SWISS-PROT protein sequence data bank and its supplement TrEMBL. *Nucleic acids research* (1997), 31–36.

[9] Satanjeev Banerjee and Alon Lavie. 2005. METEOR: An automatic metric for MT evaluation with improved correlation with human judgments. In *Proceedings of the acl workshop on intrinsic and extrinsic evaluation measures for machine translation and/or summarization*. 65–72.

[10] Helen M. Berman, John Westbrook, Zukang Feng, Gary Gilliland, T. N. Bhat, Helge Weissig, Ilya N. Shindyalov, and Philip E. Bourne. 2000. The Protein Data Bank. *Nucleic Acids Research* (2000), 235–242.

[11] Nadav Brandes, Dan Ofer, Yam Peleg, Nadav Rappoport, and Michal Linial. 2022. ProteinBERT: a universal deep-learning model of protein sequence and function. *Bioinformatics* (2022), 2102–2110.

[12] Liyi Chen, Ying Sun, Shengzhe Zhang, Yuyang Ye, Wei Wu, and Hui Xiong. 2024. Tackling Uncertain Correspondences for Multi-Modal Entity Alignment. In Proc. of NeurIPS.

[13] Liyi Chen, Panrong Tong, Zhongming Jin, Ying Sun, Jieping Ye, and Hui Xiong. 2024. Plan-on-Graph: Self-Correcting Adaptive Planning of Large Language Model on Knowledge Graphs. In Proc. of NeurIPS.

[14] Kevin Clark, Minh-Thang Luong, Quoc V Le, and Christopher D Manning. 2020. ELECTRA: Pre-training Text Encoders as Discriminators Rather Than Generators. In Proc. of ICLR.

[15] Wenliang Dai, Junnan Li, Dongxu Li, Anthony Meng Huat Tiong, Junqi Zhao, Weisheng Wang, Boyang Li, Pascale N Fung, and Steven Hoi. 2024. Instructclip: Towards general-purpose vision-language models with instruction tuning. *Proc. of NeurIPS* (2024).

[16] Zihang Dai, Zhilin Yang, Yiming Yang, Jaime G Carbonell, Quoc Le, and Ruslan Salakhutdinov. 2019. Transformer-XL: Attentive Language Models beyond a Fixed-Length Context. In Proc. of ACL. 2978–2988.

[17] DeepSeek-AI, Aixin Liu, Bei Feng, Bing Xue, et al. 2025. DeepSeek-V3 Technical Report. *arXiv:2412.19437 [cs.CL]* <https://arxiv.org/abs/2412.19437>

[18] Jacob Devlin, Ming-Wei Chang, Kenton Lee, and Kristina Toutanova. 2019. Bert: Pre-training of deep bidirectional transformers for language understanding. In Proc. of NAACL. 4171–4186.

[19] Danny Diess, Fei Xia, Mehdi SM Sajjadi, Corey Lynch, Aakanksha Chowdhery, Brian Ichter, Ayaanah Wahid, Jonathan Tompson, Quan Vuong, Tian Yu, et al. 2023. PaLM-E: an embodied multimodal language model. In Proc. of ICML. 8469–8488.

[20] Ahmed Elnaggar, Michael Heinzinger, Christian Dallago, Ghalia Rehawi, Yu Wang, Llion Jones, Tom Gibbs, Tamas Feher, Christoph Angerer, Martin Steinegger, Debsindhu Bhowmik, and Burkhard Rost. 2022. ProfTrans: Toward Understanding the Language of Life Through Self-Supervised Learning. *IEEE Transactions on Pattern Analysis and Machine Intelligence* (2022), 7112–7127.

[21] Hehe Fan, Zhangyang Wang, Yi Yang, and Mohan Kankanhalli. 2023. Continuous-Discrete Convolution for Geometry-Sequence Modeling in Proteins. In Proc. of ICLR.

[22] Yin Fang, Xiaozhuan Liang, Ningyu Zhang, Kangwei Liu, Rui Huang, Zhuo Chen, Xiaohui Fan, and Huajun Chen. 2024. Mol-Instructions: A Large-Scale Biomolecular Instruction Dataset for Large Language Models. In Proc. of ICLR.

[23] Limin Fu, Beifang Niu, Zhengwei Zhu, Sita Wu, and Weizhong Li. 2012. CD-HIT: accelerated for clustering the next-generation sequencing data. *Bioinformatics* (2012), 3150–3152.

[24] Fabian Fuchs, Daniel Worrall, Volker Fischer, and Max Welling. 2020. Se(3)-transformers: 3d roto-translation equivariant attention networks. *Proc. of NeurIPS* (2020), 1970–1981.

[25] Xinyang Geng and Hao Liu. 2023. *OpenLLaMA: An Open Reproduction of LLaMA*. [https://github.com/openlm-research/open\\_llama](https://github.com/openlm-research/open_llama)

[26] Vladimir Gligorijević, P Douglas Renfrew, Tomasz Kosciolek, Julia Koehler Leman, Daniel Berenborg, Tommi Vatanen, Chris Chandler, Bryn C Taylor, Ian M Fisk, Hera Vlamakis, et al. 2021. Structure-based protein function prediction using graph convolutional networks. *Nature communications* (2021), 3168.

[27] Jonathan Godwin, Michael Schaaerschmidt, Alexander L Gaunt, Alvaro Sanchez-Gonzalez, Yulia Rubanova, Petar Veličković, James Kirkpatrick, and Peter Battaglia. 2022. Simple GNN Regularisation for 3D Molecular Property Prediction and Beyond. In Proc. of ICLR.

[28] Yu Gu, Robert Tinn, Hao Cheng, Michael Lucas, Naoto Usuyama, Xiaodong Liu, Tristan Naumann, Jianfeng Gao, and Hoifung Poon. 2021. Domain-specific language model pretraining for biomedical natural language processing. *ACM Transactions on Computing for Healthcare (HEALTH)* (2021), 1–23.

[29] Han Guo, Mingjia Huo, and Pengtao Xie. 2023. ProteinChat: Towards Enabling ChatGPT-Like Capabilities on Protein 3D Structures. (2023).

[30] Harold Hartley. 1951. Origin of the word 'protein'. *Nature* (1951), 244–244.

[31] Thomas Hayes, Roshan Rao, Halil Akin, Nicholas J Sofroniew, Deniz Oktay, Zeming Lin, Robert Verkuil, Vincent Q Tran, Jonathan Deaton, Marius Wigert, et al. 2025. Simulating 500 million years of evolution with a language model. *Science* (2025), eads0018.

[32] Michael Heinzinger, Ahmed Elnaggar, Yu Wang, Christian Dallago, Dmitrii Nечаev, Florian Matthes, and Burkhard Rost. 2019. Modeling aspects of the language of life through transfer-learning protein sequences. *BMC bioinformatics* (2019), 1–17.

[33] Pedro Hermosilla, Marco Schäfer, Matej Lang, Gloria Fackelmann, Pere-Pau Vázquez, Barbora Kozlikova, Michael Krone, Tobias Ritschel, and Timo Ropinski. 2021. Intrinsic-Extrinsic Convolution and Pooling for Learning on 3D Protein Structures. In Proc. of ICLR.

[34] Sepp Hochreiter and Jürgen Schmidhuber. 1997. Long short-term memory. *Neural computation* (1997), 1735–1780.

[35] Chloe Hsu, Robert Verkuil, Jason Liu, Zeming Lin, Brian Hie, Tom Sercu, Adam Lerer, and Alexander Rives. 2022. Learning inverse folding from millions of predicted structures. *ICML* (2022).

[36] Bozhen Hu, Jun Xia, Jiangbin Zheng, Cheng Tan, Yufei Huang, Yongjie Xu, and Stan Z. Li. 2022. Protein Language Models and Structure Prediction: Connection and Progression. *arXiv:2211.16742 [q-bio.QM]* <https://arxiv.org/abs/2211.16742>

[37] Zhiheng Huang, Wei Xu, and Kai Yu. 2015. Bidirectional LSTM-CRF Models for Sequence Tagging. *arXiv:1508.01991 [cs.CL]* <https://arxiv.org/abs/1508.01991>

[38] Robert A. Jacobs, Michael I. Jordan, Steven J. Nowlan, and Geoffrey E. Hinton. 1991. Adaptive Mixtures of Local Experts. *Neural Computation* (1991), 79–87.

[39] Bowen Jing, Stephan Eismann, Patricia Suriana, Raphael John Lamarre Townshend, and Ron Dror. 2021. Learning from Protein Structure with Geometric Vector Perceptrons. In Proc. of ICLR.

[40] John Jumper, Richard Evans, Alexander Pritzel, Tim Green, Michael Figurnov, Olaf Ronneberger, Kathryn Tunyasuvunakool, Russ Bates, Augustin Žídek, Anna Potapenko, et al. 2021. Highly accurate protein structure prediction with AlphaFold. *Nature* (2021), 583–589.

[41] Jared Kaplan, Sam McCandlish, Tom Henighan, Tom B. Brown, Benjamin Chess, Rewon Child, Scott Gray, Alec Radford, Jeffrey Wu, and Dario Amodei. 2020. Scaling Laws for Neural Language Models. *arXiv:2001.08361 [cs.LG]* <https://arxiv.org/abs/2001.08361>

[42] Aran Komatsuzaki, Joan Puigcerver, James Lee-Thorp, Carlos Riquelme Ruiz, Basil Mustafa, Joshua Ainslie, Yi Tay, Mostafa Dehghani, and Neil Houlsby. 2023. Sparse Upcycling: Training Mixture-of-Experts from Dense Checkpoints. In Proc. of ICLR.

[43] Ben Krause, Liang Lu, Iain Murray, and Steve Renals. 2017. Multiplicative LSTM for sequence modelling. *arXiv:1609.07959 [cs.NE]* <https://arxiv.org/abs/1609.07959>

[44] Zhenzhong Lan, Mingda Chen, Sebastian Goodman, Kevin Gimpel, Piyush Sharma, and Radu Soricut. 2020. ALBERT: A Lite BERT for Self-supervised Learning of Language Representations. In Proc. of ICLR.

[45] Dmitry Lepikhin, HyoukJoong Lee, Yuanzhong Xu, Dehao Chen, Orhan Firat, Yanping Huang, Maxim Krikun, Noam Shazeer, and Zhifeng Chen. 2020. GShard: Scaling Giant Models with Conditional Computation and Automatic Sharding. In Proc. of ICLR.

[46] Junnan Li, Dongxu Li, Silvio Savarese, and Steven Hoi. 2023. Blip-2: Bootstrapping language-image pre-training with frozen image encoders and large language models. In Proc. of ICML. 19730–19742.

[47] Junnan Li, Ramprasaath Selvaraju, Akhilesh Gotmare, Shafiq Joty, Caiming Xiong, and Steven Chu Hong Hoi. 2021. Align before fuse: Vision and language representation learning with momentum distillation. *Proc. of NeurIPS* (2021), 9694–9705.

[48] Yi-Lun Liao and Tess Smidt. 2022. Equiformer: Equivariant Graph Attention Transformer for 3D Atomistic Graphs. In Proc. of ICLR.

[49] Yi-Lun Liao, Brandon Wood, Abhishek Das\*, and Tess Smidt\*. 2024. EquiFormerV2: Improved Equivariant Transformer for Scaling to Higher-Degree Representations. In *Proc. of ICLR*.

[50] Bin Lin, Zhenyu Tang, Yang Ye, Jinfa Huang, Junwu Zhang, Yatian Pang, Peng Jin, Munan Ning, Jiebo Luo, and Li Yuan. 2024. MoE-LLAva: Mixture of Experts for Large Vision-Language Models. arXiv:2401.15947 [cs.CV] <https://arxiv.org/abs/2401.15947>

[51] Chin-Yew Lin. 2004. ROUGE: A Package for Automatic Evaluation of Summaries. In *Text Summarization Branches Out*. 74–81.

[52] Zeming Lin, Halil Akin, Roshan Rao, Brian Hie, Zhongkai Zhu, Wenting Lu, Nikita Smetanin, Allan dos Santos Costa, Maryam Fazel-Zarandi, Tom Sercu, Sal Candido, et al. 2022. Language models of protein sequences at the scale of evolution enable accurate structure prediction. *bioRxiv* (2022).

[53] Zeming Lin, Halil Akin, Roshan Rao, Brian Hie, Zhongkai Zhu, Wenting Lu, Nikita Smetanin, Robert Verkuil, Ori Kabeli, Yaniv Shmueli, et al. 2023. Evolutionary-scale prediction of atomic-level protein structure with a language model. *Science* (2023), 1123–1130.

[54] Haotian Liu, Chunyuan Li, Qingyang Wu, and Yong Jae Lee. 2024. Visual instruction tuning. *Proc. of NeurIPS* (2024).

[55] Shengchao Liu, Yanjing Li, Zhuoxinran Li, Anthony Gitter, Yutao Zhu, Jiarui Lu, Zhao Xu, Weili Nie, Arvind Ramanathan, Chaowei Xiao, et al. 2025. A text-guided protein design framework. *Nature Machine Intelligence* (2025), 1–12.

[56] Zhiyuan Liu, An Zhang, Hao Fei, Enzhi Zhang, Xiang Wang, Kenji Kawaguchi, and Tat-Seng Chua. 2024. ProtT3: Protein-to-Text Generation for Text-based Protein Understanding. In *Proc. of ACL*. 5949–5966.

[57] Ilya Loshchilov and Frank Hutter. 2019. Decoupled Weight Decay Regularization. In *Proc. of ICLR*.

[58] Shengjie Luo, Tianlang Chen, Yixian Xu, Shuxin Zheng, Tie-Yan Liu, Liwei Wang, and Di He. 2023. One Transformer Can Understand Both 2D & 3D Molecular Data. In *Proc. of ICLR*.

[59] Yizhen Luo, Jiahuan Zhang, Siqi Fan, Kai Yang, Yushuai Wu, Mu Qiao, and Zaiqing Nie. 2023. BioMedGPT: Open Multimodal Generative Pre-trained Transformer for BioMedicine. arXiv:2308.09442 [cs.CE] <https://arxiv.org/abs/2308.09442>

[60] Liuzhenghao Lv, Zongying Lin, Hao Li, Yuyang Liu, Jiaxi Cui, Calvin Yu-Chian Chen, Li Yuan, and Yonghong Tian. 2024. ProLLaMA: A Protein Language Model for Multi-Task Protein Language Processing. arXiv:2402.16445 [cs.CE] <https://arxiv.org/abs/2402.16445>

[61] OpenAI, Josh Achiam, Steven Adler, Sandhini Agarwal, Lama Ahmad, Ilge Akkaya, Florencia Leoni Aleman, et al. 2024. GPT-4 Technical Report. arXiv:2303.08774 [cs.CL] <https://arxiv.org/abs/2303.08774>

[62] Long Ouyang, Jeffrey Wu, Xu Jiang, Diogo Almeida, Carroll Wainwright, Pamela Mishkin, Chong Zhang, Sandhini Agarwal, Katarina Slama, Alex Ray, et al. 2022. Training language models to follow instructions with human feedback. *Proc. of NeurIPS* (2022), 27730–27744.

[63] Qizhi Pei, Lijun Wu, Kaiyuan Gao, Xiaozhuan Liang, Yin Fang, Jinhua Zhu, Shufang Xie, Tao Qin, and Rui Yan. 2024. BioT5+: Towards Generalized Biological Understanding with IUPAC Integration and Multi-task Tuning. In *Proc. of ACL Findings*. 1216–1240.

[64] Qizhi Pei, Lijun Wu, Kaiyuan Gao, Jinhua Zhu, Yue Wang, Zun Wang, Tao Qin, and Rui Yan. 2024. Leveraging Biomolecule and Natural Language through Multi-Modal Learning: A Survey. *arXiv preprint arXiv:2403.01528* (2024). arXiv:2403.01528 [cs.CL] <https://arxiv.org/abs/2403.01528>

[65] Alec Radford, Jong Wook Kim, Chris Hallacy, Aditya Ramesh, Gabriel Goh, Sandhini Agarwal, Girish Sastry, Amanda Askell, Pamela Mishkin, Jack Clark, et al. 2021. Learning transferable visual models from natural language supervision. In *Proc. of ICML*. 8748–8763.

[66] Alec Radford, Jong Wook Kim, Chris Hallacy, Aditya Ramesh, Gabriel Goh, Sandhini Agarwal, Girish Sastry, Amanda Askell, Pamela Mishkin, Jack Clark, et al. 2021. Learning transferable visual models from natural language supervision. In *Proc. of ICML*. 8748–8763.

[67] Predrag Radivojac, Wyatt T Clark, Tal Ronnen Oron, Alexandra M Schnoes, Tobias Wittkop, Artem Sokolov, Kiley Graim, Christopher Funk, Karin Verspoor, Asa Ben-Hur, et al. 2013. A large-scale evaluation of computational protein function prediction. *Nature methods* (2013), 221–227.

[68] Colin Raffel, Noam Shazeer, Adam Roberts, Katherine Lee, Sharan Narang, Michael Matena, Yanqi Zhou, Wei Li, and Peter J Liu. 2020. Exploring the limits of transfer learning with a unified text-to-text transformer. *Journal of machine learning research* (2020), 1–67.

[69] Roshan M Rao, Jason Liu, Robert Verkuil, Joshua Meier, John Canny, Pieter Abbeel, Tom Sercu, and Alexander Rives. 2021. MSA Transformer. In *Proc. of ICML*. 8844–8856.

[70] Jeff Rasley, Samyam Rajbhandari, Olatunji Ruwase, and Yuxiong He. 2020. Deep-speed: System optimizations enable training deep learning models with over 100 billion parameters. In *Proc. of KDD*. 3505–3506.

[71] Alexander Rives, Joshua Meier, Tom Sercu, Siddharth Goyal, Zeming Lin, Jason Liu, Demi Guo, Myle Ott, C. Lawrence Zitnick, Jerry Ma, and Rob Fergus. 2021. Biological structure and function emerge from scaling unsupervised learning to 250 million protein sequences. *Proceedings of the National Academy of Sciences* (2021), e2016239118.

[72] Ronald Rosenfeld. 2000. Two decades of statistical language modeling: Where do we go from here? *Proc. IEEE* (2000), 1270–1278.

[73] B. Scholkopf, Kah-Kay Sung, C.J.C. Burges, F. Girosi, P. Niyogi, T. Poggio, and V. Vapnik. 1997. Comparing support vector machines with Gaussian kernels to radial basis function classifiers. *IEEE Transactions on Signal Processing* (1997), 2758–2765.

[74] Yu Shi, Shuxin Zheng, Guolin Ke, Yifei Shen, Jiacheng You, Jiyan He, Shengjie Luo, Chang Liu, Di He, and Tie-Yan Liu. 2023. Benchmarking Graphomer on Large-Scale Molecular Modeling Datasets. arXiv:2203.04810 [cs.LG] <https://arxiv.org/abs/2203.04810>

[75] Martin Steinegger, Miltot Mirdita, and Johannes Söding. 2019. Protein-level assembly increases protein sequence recovery from metagenomic samples many-fold. *Nature methods* (2019), 603–606.

[76] Martin Steinegger and Johannes Söding. 2018. Clustering huge protein sequence sets in linear time. *Nature communications* (2018), 2542.

[77] Nils Strothoff, Patrick Wagner, Markus Wenzel, and Wojciech Samek. 2020. UDSMProt: universal deep sequence models for protein classification. *Bioinformatics* (2020), 2401–2409.

[78] Jin Su, Chenchen Han, Yuyang Zhou, Junjie Shan, Xibin Zhou, and Fajie Yuan. 2024. SaProt: Protein Language Modeling with Structure-aware Vocabulary. In *Proc. of ICLR*.

[79] Ilya Sutskever, Oriol Vinyals, and Quoc V Le. 2014. Sequence to sequence learning with neural networks. *Proc. of NeurIPS* (2014).

[80] Baris E Suzek, Yuqi Wang, Hongzhan Huang, Peter B McGarvey, Cathy H Wu, and UniProt Consortium. 2015. UniRef clusters: a comprehensive and scalable alternative for improving sequence similarity searches. *Bioinformatics* (2015), 926–932.

[81] Ross Taylor, Marcin Kardas, Guillem Cucurull, Thomas Scialom, Anthony Hartshorn, Elvis Saravia, Andrew Poulton, Viktor Kerkez, and Robert Stojnic. 2022. Galactica: A Large Language Model for Science. arXiv:2211.09085 [cs.CL] <https://arxiv.org/abs/2211.09085>

[82] Gemini Team, Rohan Anil, Sebastian Borgeaud, Yonghui Wu, Jean-Baptiste Alayrac, Jiahui Yu, Radu Soricut, Johan Schalkwyk, Andrew M Dai, Anja Hauth, et al. 2025. Gemini: a family of highly capable multimodal models. *arXiv preprint arXiv:2312.11805* (2025). arXiv:2312.11805 [cs.CL] <https://arxiv.org/abs/2312.11805>

[83] Hugo Touvron, Louis Martin, Kevin Stone, et al. 2023. Llama 2: Open Foundation and Fine-Tuned Chat Models. arXiv:2307.09288 [cs.CL] <https://arxiv.org/abs/2307.09288>

[84] Mihaly Varadi, Stephen Anyango, Mandar Deshpande, Sreemath Nair, Cindy Natassia, Galabina Yordanova, David Yuan, Oana Stroe, Gemma Wood, Agata Laydon, et al. 2022. AlphaFold Protein Structure Database: massively expanding the structural coverage of protein-sequence space with high-accuracy models. *Nucleic acids research* (2022), D439–D444.

[85] Ashish Vaswani, Noam Shazeer, Niki Parmar, Jakob Uszkoreit, Llion Jones, Aidan N Gomez, Łukasz Kaiser, and Illia Polosukhin. 2017. Attention is all you need. *Proc. of NeurIPS* (2017).

[86] Weihan Wang, Qingsong Lv, Wenmeng Yu, Wenyi Hong, Ji Qi, Yan Wang, Junhui Ji, Zhiyong Yang, Lei Zhao, Song XiXuan, Jiazheng Xu, Kepin Chen, Bin Xu, Juanzi Li, Yuxiao Dong, Ming Ding, and Jie Tang. 2024. CogVLM: Visual Expert for Pretrained Language Models. In *Proc. of NeurIPS*.

[87] Yusong Wang, Shaoning Li, Tong Wang, Bin Shao, Nanning Zheng, and Tie-Yan Liu. 2024. Geometric Transformer with Interatomic Positional Encoding. *Proc. of NeurIPS* (2024).

[88] Zichen Wang, Steven A Combs, Ryan Brand, Miguel Romero Calvo, Panpan Xu, George Price, Nataliya Golovach, Emmanuel O Salawu, Colby J Wise, Sri Priya Ponnappalli, et al. 2022. Lm-gvp: an extensible sequence and structure informed deep learning framework for protein property prediction. *Scientific reports* (2022), 6832.

[89] Zirui Wang, Jiahui Yu, Adams Wei Yu, Zihang Dai, Yulia Tsvetkov, and Yuan Cao. 2021. SimVLM: Simple Visual Language Model Pretraining with Weak Supervision. In *Proc. of ICLR*.

[90] Zeyuan Wang, Qiang Zhang, Keyan Ding, Ming Qin, Xiang Zhuang, Xiaotong Li, and Huajun Chen. 2024. InstructProtein: Aligning Human and Protein Language via Knowledge Instruction. In *Proc. of ACL*. 1114–1136.

[91] James C. Whisstock and Arthur M. Lesk. 2003. Prediction of protein function from protein sequence and structure. *Quarterly Reviews of Biophysics* (2003), 307–340.

[92] Lirong Wu, Yufei Huang, Haitao Lin, and Stan Z. Li. 2022. A Survey on Protein Representation Learning: Retrospect and Prospect. arXiv:2301.00813 [cs.LG] <https://arxiv.org/abs/2301.00813>

[93] Wei Wu, Zhuoshi Pan, Chao Wang, Liyi Chen, Yunchu Bai, Tianfu Wang, Kun Fu, Zheng Wang, and Hui Xiong. 2025. TokenSelect: Efficient Long-Context Inference and Length Extrapolation for LLMs via Dynamic Token-Level KV Cache Selection. arXiv:2411.02886 [cs.CL] <https://arxiv.org/abs/2411.02886>

[94] Wei Wu, Chao Wang, Dazhong Shen, Chuan Qin, Liyi Chen, and Hui Xiong. 2024. AFDGCF: Adaptive Feature De-correlation Graph Collaborative Filtering for Recommendations. In Proc. of SIGIR. 1242–1252.

[95] Zonghan Wu, Shirui Pan, Fengwen Chen, Guodong Long, Chengqi Zhang, and Philip S Yu. 2020. A comprehensive survey on graph neural networks. *IEEE transactions on neural networks and learning systems* (2020), 4–24.

[96] Congxi Xiao, Jingbo Zhou, Jizhou Huang, Tong Xu, and Hui Xiong. 2023. Spatial heterophily aware graph neural networks. In *Proceedings of the 29th ACM SIGKDD conference on knowledge discovery and data mining*. 2752–2763.

[97] Congxi Xiao, Jingbo Zhou, Yixiong Xiao, Jizhou Huang, and Hui Xiong. 2024. ReFound: Crafting a Foundation Model for Urban Region Understanding upon Language and Visual Foundations. In *Proceedings of the 30th ACM SIGKDD Conference on Knowledge Discovery and Data Mining*. 3527–3538.

[98] Minghao Xu, Xinyu Yuan, Santiago Miret, and Jian Tang. 2023. Protst: Multi-modality learning of protein sequences and biomedical texts. In Proc. of ICML. 38749–38767.

[99] Zhihan Yang, Zihang Dai, Yiming Yang, Jaime Carbonell, Russ R Salakhutdinov, and Quoc V Le. 2019. Xlnet: Generalized autoregressive pretraining for language understanding. Proc. of NeurIPS (2019).

[100] Qinghao Ye, Haiyang Xu, Guohai Xu, Jiabo Ye, Ming Yan, Yiyang Zhou, Junyang Wang, Anwen Hu, Pengcheng Shi, Yaya Shi, et al. 2024. mPLUG-Owl: Modularization Empowers Large Language Models with Multimodality. arXiv preprint arXiv:2304.14178 (2024). arXiv:2304.14178 [cs.CL] <https://arxiv.org/abs/2304.14178>

[101] Shukang Yin, Chaoyou Fu, Sirui Zhao, Ke Li, Xing Sun, Tong Xu, and Enhong Chen. 2024. A survey on multimodal large language models. *National Science Review* (2024), nwae403.

[102] Yong Yu, Xiaosheng Si, Changhua Hu, and Jianxun Zhang. 2019. A review of recurrent neural networks: LSTM cells and network architectures. *Neural computation* (2019), 1235–1270.

[103] Sheheryar Zaidi, Michael Schaarschmidt, James Martens, Hyunjik Kim, Yee Whye Teh, Alvaro Sanchez-Gonzalez, Peter Battaglia, Razvan Pascanu, and Jonathan Godwin. 2023. Pre-training via Denoising for Molecular Property Prediction. In Proc. of ICLR.

[104] Ningyu Zhang, Zhen Bi, Xiaozhuan Liang, Siyuan Cheng, Haosen Hong, Shumin Deng, Qiang Zhang, Jiazhang Liang, and Huajun Chen. 2022. OntoProtein: Protein PreTraining With Gene Ontology Embedding. In Proc. of ICLR.

[105] Peiyuan Zhang, Guangtao Zeng, Tianduo Wang, and Wei Lu. 2024. TinyLlama: An Open-Source Small Language Model. arXiv:2401.02385 [cs.CL] <https://arxiv.org/abs/2401.02385>

[106] Shengzhe Zhang, Liyi Chen, Dazhong Shen, Chao Wang, and Hui Xiong. 2025. Hierarchical Time-Aware Mixture of Experts for Multi-Modal Sequential Recommendation. In *Proceedings of the ACM on Web Conference 2025*. 3672–3682.

[107] Tianyi Zhang\*, Varsha Kishore\*, Felix Wu\*, Kilian Q. Weinberger, and Yoav Artzi. 2020. BERTScore: Evaluating Text Generation with BERT. In Proc. of ICLR.

[108] Zuobai Zhang, Chuanrui Wang, Minghao Xu, Vijil Chenthamarakshan, Aurélie Lozano, Payel Das, and Jian Tang. 2023. A Systematic Study of Joint Representation Learning on Protein Sequences and Structures. arXiv:2303.06275 [q-bio.QM] <https://arxiv.org/abs/2303.06275>

[109] Zuobai Zhang, Minghao Xu, Arian Rokkum Jamasb, Vijil Chenthamarakshan, Aurélie Lozano, Payel Das, and Jian Tang. 2023. Protein Representation Learning by Geometric Structure Pretraining. In Proc. of ICLR.

[110] Wayne Xin Zhao, Kun Zhou, Junyi Li, et al. 2025. A Survey of Large Language Models. arXiv:2303.18223 [cs.CL] <https://arxiv.org/abs/2303.18223>

[111] Gengmo Zhou, Zhifeng Gao, Qiankun Ding, Hang Zheng, Hongteng Xu, Zhemwei Wei, Linfeng Zhang, and Guolin Ke. 2023. Uni-Mol: A Universal 3D Molecular Representation Learning Framework. In Proc. of ICLR.

[112] Deyao Zhu, Jun Chen, Xiaolian Shen, Xiang Li, and Mohamed Elhoseiny. 2024. MiniGPT-4: Enhancing Vision-Language Understanding with Advanced Large Language Models. In Proc. of ICLR.

[113] Barret Zoph, Irwan Bello, Sameer Kumar, Nan Du, Yanping Huang, Jeff Dean, Noam Shazeer, and William Fedus. 2022. ST-MoE: Designing Stable and Transferable Sparse Expert Models. arXiv:2202.08906 [cs.CL] <https://arxiv.org/abs/2202.08906>

## A Supplement to Related Work

**Multimodal Instruction Tuning.** With the emergence of Multimodal LLMs (MLLMs) such as GPT4 [61] and Genimi [82], MLLMs have become a focal point of research. Initially, works like CLIP [65], ALBEF [47], VLMo [66], SimVLM [89] emphasized exploring the cross-modal alignment [12] between vision and language. Subsequently, based on modal alignment, Flamingo [3] and BLIP2 [46] established bridges between visual encoders and LLMs using the Perceiver Resampler and the Q-Former, respectively. Following this, PaLM-E [19] introduced "multimodal sentences" as input, injecting real-world continuous sensor data into the LLMs in the form of language tokens, thereby endowing the model with a general multi-task capability. Additionally, efforts such as InstructBLIP [15], LLaVA [54], MiniGPT4 [112], mPLUGOwl [100], Qwen-VL [7], CogVLM [86] applied the crucial instruction tuning technique from LLMs to MLLMs, enhancing the MLLMs' ability to follow multimodal instructions. At the same time, they introduced innovations from the perspectives such as the instruction construction, training paradigms, and model design, which in turn refreshed the performance of MLLMs in a variety of visual-language downstream tasks [101]. In this paper, we attempt to apply this paradigm to the protein domain, investigating the potential of endowing LLMs with general-purpose protein understanding capabilities.

**Learning with 3D Structural Information.** Although pLMs pre-trained on protein sequences have been proven to be effective in numerous tasks, the protein structure is inherently a determinant of protein function [5, 30]. More effectively utilizing 3D structural information can help to understand proteins more comprehensively. To capture the impact of geometric positioning and interaction relationships among residues, a class of methods that encode 3D geometric information into rotation-invariant scalars, which was then processed through graph neural networks (GNNs) [13, 94–96] for message passing [92, 108]. For example, IEConv[33] utilized a multi-graph to depict primary and secondary structures through covalent and hydrogen bonds and represented the tertiary structure with the spatial 3D coordinates of atoms. By blending intrinsic and extrinsic node distances and employing hierarchical pooling, it effectively perceived all three structural levels of proteins. GearNet went further by incorporating three types of directed edges (sequential edges, radius edges and k-NN edges) into the graph, capturing information at various structural levels. On this basis, CDCConv [21] attempted to parameterize the kernel matrices using MLP, as opposed to employing distinct kernel matrices for varying edge types, which enabled a more flexible and efficient modeling of complex interactions between residues. Additionally, another class of methods sought to prevent the loss of 3D structural information by incorporating 3D rigid transformations into the network operations. This led to the development of geometric GNNs/Transformers characterized by SE(3) invariance and equivariance [24, 48, 49, 58, 87, 111]. Representative examples of this approach, such as GVP [39] and EvoFormer [40], were utilized by ESM-IF [35], AlphaFold2 [40], respectively. Furthermore, to leverage information from both evolutionary-scale protein sequences and the relatively limited protein structures, some other methods [88, 108] attempted to establish a connection between these two types of data.

## B Construction of Protein Instruction Dataset

Currently, the widely recognized protein-text paired databases in the protein domain mainly include Swiss-Prot, TrEMBL [8], and RCSB PDB [10], with their specific contents detailed in Table 8. Since most of the text content in TrEMBL comes from automatic annotation methods, to eliminate the impact of its unreliability on the main experiments, unless otherwise specified, this paper only uses protein-text information from Swiss-Prot and RCSB PDB databases. The corresponding structures are from AlphaFoldDB [84] and experimentally determined structures in RCSB PDB. The statistical information about the complete protein instruction dataset is shown in Table 9 and Figure 4.

The instruction template and example responses for Swiss-Prot are as follows:

### • Function

- What is the primary function of <protein>?
- What is the main function of <protein>?
- What is the function of <protein>?
- Explain the function of <protein>.
- What is the characteristic function associated with the protein <protein>?
- Can you define the function profile of the <protein>?
- Give me the function caption of <protein>.

**Example Response** Binds to muscle nicotinic acetylcholine receptor (nAChR) and inhibit acetylcholine from binding to the receptor, thereby impairing neuromuscular transmission. Produces peripheral paralysis by blocking neuromuscular transmission at the postsynaptic site. Has a lower toxicity than cobrotoxin.

### • Similarity

- Which protein family does <protein> belong to?
- What is the protein family of <protein>?
- What is the closest related protein family for <protein>?
- Can you identify the family or group that <protein> belongs to?
- To which protein family <protein> is classified?
- Which protein class does <protein> fall into?

**Example Response** Belongs to the snake three-finger toxin family. Short-chain subfamily. Aminergic toxin sub-subfamily.

### • Subcellular location

- Where is <protein> located in the cell?
- Can you specify the subcellular location of <protein>?
- What is the subcellular location of <protein>?
- Could you describe the subcellular location of <protein>?
- What are the primary subcellular regions where <protein> is detected?

**Example Response** Colocalizes with ENA/VASP proteins at lamellipodia tips and focal adhesions, and F-actin at the leading edge. At the membrane surface, associates, via the PH domain, preferentially with the inositol phosphates, PtdIns(5)P and PtdIns(3)P. This binding appears to be necessary for the efficient interaction of the RA domain to Ras-GTPases (By similarity).

### • Induction

- Description the effects of environmental factors of <protein>’s expression.

- What are the environmental factors that induce the expression of <protein>?

- What environmental factors causes the upregulation of <protein>?
- What are the environmental factors that lead to the upregulation of <protein>?

**Example Response** Is slightly up-regulated when the bacterium is grown on t4LHyp or t3LHyp as sole carbon source.

### • Gene Ontology(Molecular Function)

- Which GO molecular function terms have <protein> been assigned to?
- What molecular function is associated with <protein>?
- Which GO terms outline the functional capabilities of <protein>?
- What are the molecular functions of <protein>?

**Example Response** ATP binding; protein serine kinase activity; protein serine/threonine kinase activity

### • Gene Ontology(Biological Process)

- Which GO biological process terms have <protein> been assigned to?
- What biological process is associated with <protein>?
- Which GO terms outline the biological processes of <protein>?
- What biological processes is <protein> involved in, based on gene ontology annotations?
- What are the biological processes of <protein>?

**Example Response** organic acid transmembrane transport; suberin biosynthetic process

### • Gene Ontology(Cellular Component)

- Which GO cellular component terms have <protein> been assigned to?
- What cellular component is associated with <protein>?
- Which GO terms outline the cellular components of <protein>?
- What cellular components is <protein> involved in, based on gene ontology annotations?
- What are the cellular components of <protein>?

**Example Response** cytosol; plant-type vacuole; plasma membrane

### • Developmental Stage

- At which specific developmental stages is <protein> expressed?
- What are the developmental stages where <protein> is expressed?
- What are the developmental stages where <protein> is detected?
- What are the developmental stages where <protein> is found?

**Example Response** Detected at high levels at the tube tip during early pollen germination. In germinated pollen tubes it is localized in a punctate pattern throughout the cytoplasm but most prominently at the tip region.

### • Short Sequence Motif

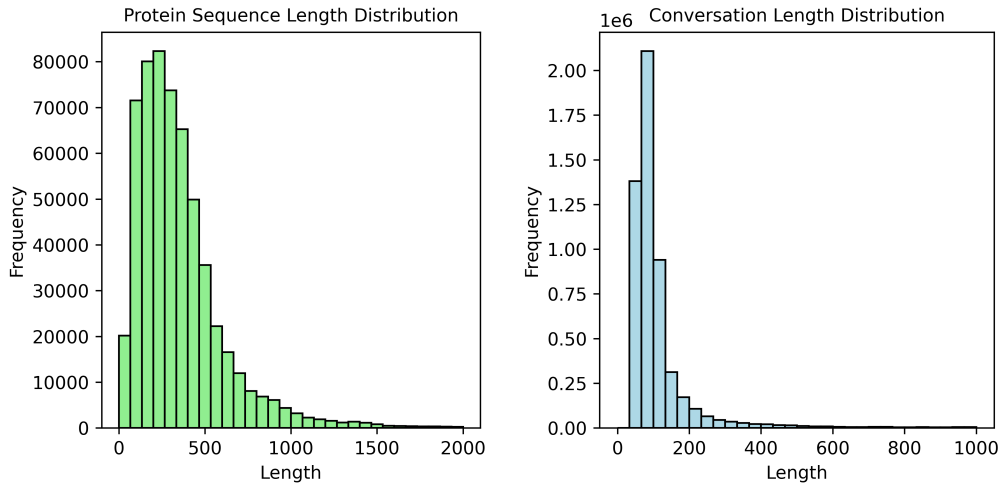
- Can you identify and list all the motifs that are predicted to be present in <protein>?
- What are the short sequence motifs that are predicted to be present in <protein>?
- What are the short sequence motifs that are present in <protein>?

**Table 8: Protein-text paired database.**

Database	Content of Related Text	# Protein	Structure
Swiss-Prot	Manually calibrated structured annotations	571,282	AlphaFoldDB
TrEMBL	Automatic structured annotation	248,234,451	N/A
RCSB PDB	Publication about protein / Meta data of protein	204,826	Experimentally-determined

**Table 9: Statistical information about the protein instruction dataset.**

Response Type	Data Source	Question Type	# Train Instructions	# Test Instructions
Open-ended Generation	Swiss-Prot	Specific property or function	2,487,543	11,911
	RCSB PDB	Protein caption	125,703	2,500
Closed-set Answer	RCSB PDB	Specific property or function	1,131,327	22,500
	GO-BP	Biological process	601,381	24,162
	GO-MF	Molecular function	391,859	5,891
	GO-CC	Cellular component	327,780	6,735
	EC	Enzymatic catalytic activity	165,695	2,278
# All Instructions			5,231,288	75,977
# Supplemental Instructions (from TrEMBL)			+ 5,253,440	N/A

**Figure 4: Distribution of protein sequence length and conversation length in the protein instruction dataset (training set).**

- What are the short sequence motifs that are found in <protein>?

**Example Response** Nucleotide carrier signature motif

- **Tissue Specificity**

- In which tissues is the expression of <protein> absent?
- Describe the tissue-specific expression pattern of <protein>?
- What is the tissue-specific expression pattern of <protein>?
- What are the tissues where <protein> is expressed?

**Example Response** Expressed in the ciliated cells of the airway epithelium. Not detected in the mucous cells.

- **Activity Regulation**

- Describe the activity regulatory mechanism of <protein> associated enzymes, transporters, microbial transcription factors.

- What is the activity regulatory mechanism of <protein>?
- Tell me about the activity regulatory mechanism of <protein>.

**Example Response** Activity is sensitive to salt concentration, a high concentration of KCl (500 mM) is needed for complete inactivation.

- **Pathway**

- What is the role of <protein> in the metabolic pathway?
- Which metabolic pathway does <protein> associate with?
- What is the metabolic pathway that <protein> is involved in?

**Example Response** Ketone degradation; acetoain degradation.

The instruction template and example responses for RCSB PDB are as follows, where {GO} and {EC} are replaced with their actual meanings (text) corresponding to GO and EC annotations.

- **Caption**

- Tell me about this protein <protein>.
- Give me some information about <protein>.
- Give me the abstract of <protein>.
- Give me a comprehensive description of <protein>.
- Tell me about <protein>.

**Example Response** The FANCM/FAAP24 heterodimer has distinct functions in protecting cells from complex DNA lesions such as interstrand crosslinks. These functions rely on the biochemical activity of FANCM/FAAP24 to recognize and bind to damaged DNA or stalled replication forks...

- **Others**

- Does this protein contain non-polymer entities, <protein>?
- Does this protein contain polymer entities, <protein>?
- Does this protein contain DNA polymer entities, <protein>?
- Does this protein contain RNA polymer entities, <protein>?
- Does this protein contain solvent entities, <protein>?
- Does this protein contain branched entities, <protein>?
- Does this protein have unmodeled polymer monomers, <protein>?
- Does this protein have hybrid nucleic acid polymer entities, <protein>?
- Does this protein have cis-peptide linkages, <protein>?

**Example Response** Yes./No.

The instruction template and example responses for other closed-set answer tasks are as follows:

- **EC**

- Does <protein> associate with enzyme classification "<EC>"?
- Does EC term "<EC>" outline the enzyme classifications of <protein>?
- Is <protein> involved in enzyme classification "<EC>"?

**Example Response** Yes./No.

- **GO-BP**

- Does <protein> associate with biological process "<GO>"?
- Does GO term "<GO>" outline the biological processes of <protein>?
- Is <protein> involved in biological process "GO"?

**Example Response** Yes./No.

- **GO-CC**

- Does <protein> associate with cellular component "<GO>"?
- Does GO term "<GO>" outline the cellular components of <protein>?
- Is <protein> involved in cellular component "<GO>"?

**Example Response** Yes./No.

- **GO-MF**

- Does <protein> associate with molecular function "<GO>"?
- Does GO term "<GO>" outline the functional capabilities of <protein>?
- Does <protein> have molecular function "<GO>"?

**Example Response** Yes./No.

## C Supplement to the Experiments

### C.1 Implementation Details

As depicted in Figure 2, we extensively utilize group learning rates throughout the entire training pipeline of SEPI. We tend to assign higher learning rates to randomly initialized parameters, while opting for lower learning rates for pre-trained parameters in order to mitigate forgetting, setting the ratio between lower and higher learning rates at 0.1. In Stage 0, we actually employ ESM2-650M [53] as the pLM and PubMedBert [28] as the text encoder (Bio-BERT) to better encode biomedical text. We set the number of Gaussian Basis Kernels to 128. In Stage 1, we choose the representation from the penultimate layer of the protein encoder as input to LLMs to minimize the discrepancy between pre-training tasks and the current task. For the LLMs, we opt for TinyLlama-1.1B [105]. In Stage 2, we continue most of the settings from Stage 1, while setting the number of experts to 4, with Top-1 expert being activated at a time. At this stage, our protein encoder is frozen. Regarding the hyper-parameter settings for SEPI-TinyLlama-MoEs, we set higher learning rate to  $5e^{-5}$  and trained for 5 epochs in Stage 0. In Stage 1, we set higher learning rate to  $2e^{-5}$  and trained for 1 epoch. In Stage 2, we set higher learning rate to  $5e^{-5}$  and trained for 1 epoch. For all stages, we trained on 32 Tesla V100 GPUs, with a batch size per GPU set to 4, employing a warm-up and linear decay learning rate scheduler, and set the warm-up ratio to 0.06. In all experiments, we employ AMP, Zero Optimizer [70] based on AdamW [57] and gradient checkpointing. For the hyper-parameter settings of other models, see Table 11. For all MoE models, we implement them based on DeepSpeed-MoE, employing expert parallelism during the training process and setting the expert parallel size to 4.

For the API-based models, we have tallied the number of tokens consumed in the experiments conducted for this paper. It is worth noting that due to the high cost associated with GPT-4 API requests, we randomly sampled 5% of the examples from the test set for testing. The specific token consumption is shown in Table 10. For all other models, we present the training hyper-parameter settings in Table 11, their training costs in Table 12, and their inference costs in Table 13.

**Table 10: Tokens consumed by API-based models.**

API Model	Token Consumption
GPT-3.5-turbo	~19M
Claude-3-haiku	~19M
GPT-4-turbo	~0.95M *
GPT-4o-mini	~19M
GPT-4o	~0.95M *
DeepSeek-V3	~19M

Table 11: Hyper-parameters of all models.

Trained Model	Epochs	Wram-up Ratio	Batch Size per GPU	Global Batch Size	(Higher) Learning Rate	Auxiliary Loss Coefficient	Optimizer Stage
TinyLlama-Chat	1	0.06	8	256	$2e^{-5}$	N/A	Zero 1
OpenLlama-v2	1	0.06	8	512	$4e^{-5}$	N/A	Zero 3
Llama-Chat	1	0.06	6	192	$2e^{-5}$	N/A	Zero 3
PIT-Stage 0	5	0.06	4	128	$2e^{-5}$	N/A	Zero 3
PIT-TinyLlama-Stage 1	1	0.06	4	128	$5e^{-5}$	N/A	Zero 2
PIT-TinyLlama-Stage 2	1	0.06	4	128	$2e^{-5}$	N/A	Zero 2
PIT-TinyLlama-MoEs-Stage 2	1	0.06	4	256	$1e^{-4}$	0.01	Zero 2
SEPI-T-Stage 0	5	0.06	4	128	$2e^{-5}$	N/A	Zero 3
SEPI-T-Llama-Stage 1	1	0.06	2	128	$5e^{-5}$	N/A	Zero 3
SEPI-T-TinyLlama-Stage 1	1	0.06	4	128	$5e^{-5}$	N/A	Zero 2
SEPI-T-TinyLlama-Stage 2	1	0.06	4	128	$2e^{-5}$	N/A	Zero 2
SEPI-T-Llama-Stage 2	1	0.06	2	128	$2e^{-5}$	N/A	Zero 3
SEPI-T-TinyLlama-MoEs-Stage 2	1	0.06	4	128	$5e^{-5}$	0.01	Zero 2

Table 12: Training cost of all models.

Trained Model	Parameter Size	Trainable Parameters	GPUs Cost (Hrs. $\times$ # V100)
TinyLlama-Chat	1.1B	1.1B	$44 \times 32$
OpenLlama-v2	3B	3B	$45 \times 64$
Llama-Chat	7B	7B	$170 \times 32$
PIT-Stage 0	650M + 110M	650M	$20 \times 32$
PIT-TinyLlama-Stage 1	1.1B + 650M	1.1B + 650M	$20 \times 32$
PIT-TinyLlama-Stage 2	1.1B + 650M	1.1B	$50 \times 32$
PIT-TinyLlama-MoEs-Stage 2	3.2B + 650M	3.2B	$68 \times 64$
SEPI-T-Stage 0	650M + 110M	650M	$26 \times 32$
SEPI-T-Llama-Stage 1	7B + 650M	7B	$82 \times 64$
SEPI-T-TinyLlama-Stage 1	1.1B + 650M	1.1B	$30 \times 32$
SEPI-T-TinyLlama-Stage 2	1.1B + 650M	1.1B	$50 \times 32$
SEPI-T-Llama-Stage 2	7B + 650M	7B	$220 \times 64$
SEPI-T-TinyLlama-MoEs-Stage 2	3.2B + 650M	3.2B	$126 \times 32$

**Table 13: Inference cost of main models.**

Inferenced Model	Parameter Size	Activated Parameters	GPUs Cost (Hrs. × # T4)
TinyLlama-Chat	1.1B	1.1B	1 × 8
OpenLlama-v2	3B	3B	8 × 8
Llama-Chat	7B	7B	11 × 8
PIT-TinyLlama	1.1B + 650M	1.1B + 650M	1.25 × 8
PIT-TinyLlama-MoEs	3.2B + 650M	1.1B + 650M	1.5 × 8
SEPI-TinyLlama	1.1B + 650M	1.1B + 650M	1.5 × 8
SEPI-TinyLlama	7B + 650M	7B + 650M	21 × 8
SEPI-TinyLlama-MoEs	3.2B + 650M	1.1B + 650M	1.75 × 8

## C.2 Metric Explanation

**BLEU Score.** The Bilingual Evaluation Understudy Score [79] (BLEU score) is a metric used to evaluate the quality of machine-translated text against human-translated reference texts, which is calculated using n-gram precision. The general formula for calculating BLEU score is as follows, where BP penalize overly short translations:

$$p_n = \frac{\sum_{C \in \{\text{Candidates}\}} \sum_{\text{n-gram} \in C} \text{Count}_{\text{clip}}(\text{n-gram})}{\sum_{C' \in \{\text{Candidates}\}} \sum_{\text{n-gram}' \in C'} \text{Count}(\text{n-gram}')}, \quad (16)$$

$$\text{BP} = \begin{cases} 1 & \text{if } c > r \\ e^{(1-r/c)} & \text{if } c \leq r \end{cases}, \quad (17)$$

$$\text{BLEU} = \text{BP} \cdot \exp \left( \sum_{n=1}^N w_n \log p_n \right), \quad (18)$$

$$\log \text{BLEU} = \min(1 - \frac{r}{c}, 0) + \sum_{n=1}^N w_n \log p_n. \quad (19)$$

**ROUGE-N Score.** ROUGE-N [51] is a widely-used automatic text evaluation metric designed to compare the similarity between generated text and reference text, which can be considered an improved version of BLEU with a focus on recall rather than precision. The general formula for calculating ROUGE score is as follows:

$$\text{ROUGE - N} = \frac{\sum_{C \in \{\text{Candidates}\}} \sum_{\text{n-gram} \in C} \text{Count}_{\text{match}}(\text{n-gram})}{\sum_{C' \in \{\text{Candidates}\}} \sum_{\text{n-gram}' \in C'} \text{Count}(\text{n-gram}')}. \quad (20)$$

**ROUGE-L Score.** ROUGE-L [51] computes the overlap of the longest common subsequence (LCS) between the produced text and the standard references as follows, where  $X$  represents the standard answer, and  $Y$  denotes the generated answer, with their respective lengths being  $n$  and  $m$ .  $\beta$  is a hyper-parameter used to adjust the focus between precision  $P_{\text{lcs}}$  and recall  $R_{\text{lcs}}$ :

$$R_{\text{lcs}} = \frac{\text{LCS}(X, Y)}{m}, \quad (21)$$

$$P_{\text{lcs}} = \frac{\text{LCS}(X, Y)}{n}, \quad (22)$$

$$\text{ROUGE - L} = \frac{(1 + \beta^2)R_{\text{lcs}}P_{\text{lcs}}}{R_{\text{lcs}} + \beta^2P_{\text{lcs}}}. \quad (23)$$

**METEOR Score.** METEOR [9] addresses certain inherent shortcomings of the BLEU score by taking into account both precision and recall evaluated over the entire corpus. The general formula for calculating METEOR score is as follows, where Penalty is the penalty of excessive word mismatches and  $\alpha$  is a hyper-parameter:

$$F = \frac{(\alpha^2 + 1)P}{R + \alpha P}, \quad (24)$$

$$\text{METEOR} = (1 - \text{Penalty}) \cdot F. \quad (25)$$

**BERT Score.** BERT score [107] is an automatic evaluation metric for text generation, which computes a similarity score for each token in the candidate sentence with each token in the reference sentence. The general formula for calculating BERT score is as follows, where tokens of reference sentence  $x$  and candidate sentence  $\hat{x}$  are represented by contextual embeddings:

$$R_{\text{BERT}} = \frac{1}{|x|} \sum_{x_i \in x} \max_{\hat{x}_j \in \hat{x}} \mathbf{x}_i^\top \hat{\mathbf{x}}_j, \quad (26)$$

$$P_{\text{BERT}} = \frac{1}{|\hat{x}|} \sum_{\hat{x}_j \in \hat{x}} \max_{x_i \in x} \mathbf{x}_i^\top \hat{\mathbf{x}}_j, \quad (27)$$

$$F_{\text{BERT}} = 2 \frac{P_{\text{BERT}} \cdot R_{\text{BERT}}}{P_{\text{BERT}} + R_{\text{BERT}}}. \quad (28)$$

## C.3 More Ablation Studies

For the data ablation experiments, we also tested different forms of protein inputs, with the results shown in Table 14. For both forms of protein inputs, the addition of extra low-quality data does not result in performance improvement but leads to performance degradation.

## C.4 More Case Studies

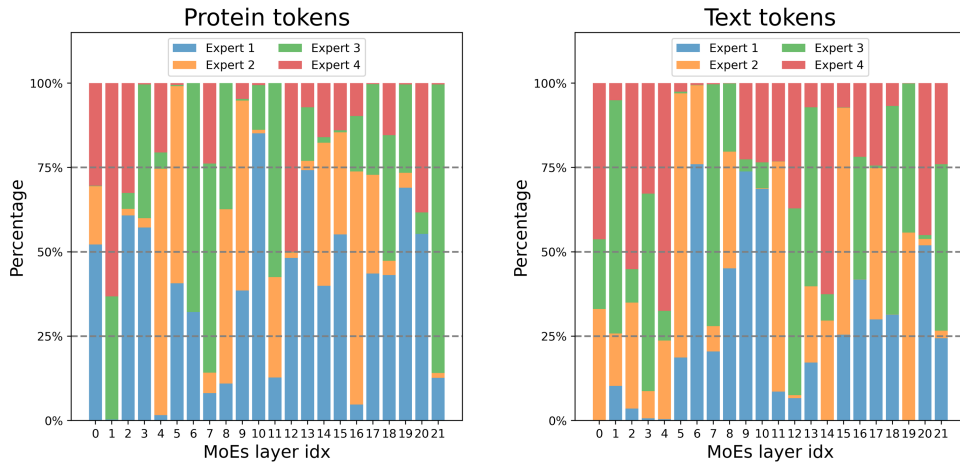
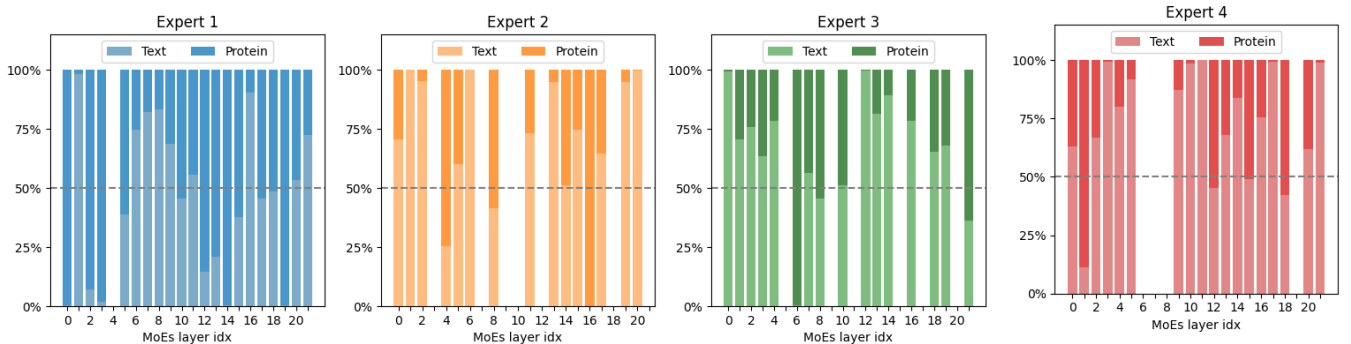
**More Visualization for Workload of Experts in SEPI.** More visualization for workload of experts in SEPI is shown in Figure 5 and 6. The results are similar to our analysis in the main text.

**More Cases for General-Purpose Protein Understanding Ability of SEPI.** More examples of our proposed SEPI-TinyLlama-MoEs are shown below:

- **O43143 (Swiss-Prot)**
  - **Instruction:** What are the short sequence motifs that are present in <protein>?
  - **Ground Truth:** DEAH box
  - **Response:** DEAH box
- **Q8DPM9 (Swiss-Prot)**
  - **Instruction:** What is the function of <protein>?
  - **Ground Truth:** Bidirectionally degrades single-stranded DNA into large acid-insoluble oligonucleotides, which are then degraded further into small acid-soluble oligonucleotides.
  - **Response:** Bidirectionally degrades single-stranded DNA into large acid-insoluble oligonucleotides, which are then degraded further into small acid-soluble oligonucleotides.
- **B4LM02 (Swiss-Prot)**
  - **Instruction:** Give me the function caption of <protein>.

**Table 14: Data ablation study on SEPIT’s pre-train data.**

Dataset	Infer w/ Struct.	Open-ended Generation				Closed-set Answer
		BLEU-2	ROUGE-L	METEOR	BERT-F1	
Protein Instrcution Dataset (5.47M)	✓	60.28	71.13	68.27	95.64	79.73%
	✗	59.98	70.87	68.00	95.59	79.53%
w/ TrEMBL (+5.25M)	✓	58.71	69.65	66.93	95.42	79.52%
	✗	58.55	69.54	66.78	95.40	79.48%

**Figure 5: Workload of experts in SEPIT for protein tokens and text tokens.****Figure 6: Workload of each expert in SEPIT for protein tokens and text tokens.**

- **Ground Truth:** Plays a central role in 2-thiolation of mcm(5) S(2)U at tRNA wobble positions of tRNA(Lys), tRNA(Glu) and tRNA(Gln). Directly binds tRNAs and probably acts by catalyzing adenylation of tRNAs, an intermediate required for 2-thiolation. It is unclear whether it acts as a sulfurtransferase that transfers sulfur from thiocarboxylated URM1 onto the uridine of tRNAs at wobble position.
- **Response:** Plays a central role in 2-thiolation of mcm(5) S(2)U at tRNA wobble positions of tRNA(Lys), tRNA(Glu) and tRNA(Gln). May act by forming a heterodimer with ctu1/atpb3 that ligates sulfur from thiocarboxylated urm1 onto the uridine of tRNAs at wobble position.
- **Q98QW4 (Swiss-Prot)**
  - **Instruction:** Which protein family does <protein> belong to?
  - **Ground Truth:** In the N-terminal section; belongs to the phosphoglycerate kinase family.
  - **Response:** Belongs to the phosphoglycerate kinase family.
- **P0DMD4 (Swiss-Prot)**
  - **Instruction:** Which protein family does <protein> belong to?
  - **Ground Truth:** Belongs to the scolopendra neurotoxin 10 family.
  - **Response:** Belongs to the scolopendra neurotoxin 02 (Dtx-II) family.
- **A1VKS2 (Swiss-Prot)**
  - **Instruction:** What is the closest related protein family for <protein>?
  - **Ground Truth:** Belongs to the pantothenate synthetase family.
  - **Response:** Belongs to the pantothenate synthetase family.
- **P67911 (Swiss-Prot)**
  - **Instruction:** What molecular function is associated with <protein>?
  - **Ground Truth:** ADP-glyceromanno-heptose 6-epimerase activity; NADP binding
  - **Response:** ADP-glyceromanno-heptose 6-epimerase activity; NADP binding
- **Q9X5Y0 (Swiss-Prot)**
  - **Instruction:** What cellular component is associated with <protein>?
  - **Ground Truth:** bacterial-type flagellum basal body
  - **Response:** bacterial-type flagellum basal body

## C.5 More Analysis

**Analysis of Error Patterns.** First, we present cases of SEPIT-TinyLlama-MoEs under major problem categories, with underlined text indicating differences from the ground truth (note that these differences are not necessarily errors). For each type, we attempt to demonstrate possible error patterns that might occur.

### Function

- **Instruction:** Explain the function of <protein>. (A5FQQ5)
  - **Response:** This protein promotes the GTP-dependent binding of aminoacyl-tRNA to the A-site of ribosomes during protein biosynthesis.

- **Ground Truth:** This protein promotes the GTP-dependent binding of aminoacyl-tRNA to the A-site of ribosomes during protein biosynthesis.
- **Instruction:** Give me the function caption of <protein>. (P44603)
  - **Response:** Catalyzes the transfer of an acyl group from acyl-phosphate (acyl-PO(4)) to glycerol-3-phosphate (G3P) to form lysophosphatidic acid (LPA). This enzyme utilizes acyl-phosphate as fatty acyl donor, but not acyl-CoA or acyl-ACP.
  - **Ground Truth:** Catalyzes the transfer of an acyl group from acyl-phosphate (acyl-PO(4)) to glycerol-3-phosphate (G3P) to form lysophosphatidic acid (LPA). This enzyme utilizes acyl-phosphate as fatty acyl donor, but not acyl-CoA or acyl-ACP.
- **Instruction:** Can you define the function profile of the <protein>? (B0BN86)
  - **Response:** Plays an essential role in mitochondrial morphogenesis.
  - **Ground Truth:** Plays a role in mitochondrial morphogenesis.

### Similarity

- **Instruction:** Which protein family does <protein> belong to? (Q99PZ1)
  - **Response:** Belongs to the 4-hydroxy-2-oxovalerate aldolase family.
  - **Ground Truth:** Belongs to the 4-hydroxy-2-oxovalerate aldolase family.
- **Instruction:** Which protein class does <protein> fall into? (A8IQE0)
  - **Response:** Belongs to the CCDC40 family.
  - **Ground Truth:** Belongs to the CCDC39 family.
- **Instruction:** To which protein family <protein> is classified? (P58600)
  - **Response:** Belongs to the UDP-N-acetylglucosamine-2-epimerase family.
  - **Ground Truth:** Belongs to the UDP-N-acetylglucosamine 2-epimerase family.

### Subcellular location

- **Instruction:** Where is <protein> located in the cell? (B0KZ78)
  - **Response:** Loosely associated with the inner membrane.
  - **Ground Truth:** Loosely associated with the inner membrane.
- **Instruction:** Could you describe the subcellular location of <protein>? (Q5M7N9)
  - **Response:** Localizes to endoplasmic reticulum-plasma membrane contact sites (EPCS). Recruited to the cell surface via the third C2 domain.
  - **Ground Truth:** Localizes to endoplasmic reticulum-plasma membrane contact sites (EPCS). Recruited to the cell membrane via the third C2 domain.
- **Instruction:** What is the subcellular location of <protein>? (Q9BXH1)
  - **Response:** Localized to the mitochondria in order to induce cytochrome c release.
  - **Ground Truth:** Localized to the mitochondria in order to induce cytochrome c release.

### Induction

- **Instruction:** Describe the effects of environmental factors of <protein>'s expression. (P66808)

- **Response:** By heat shock.
- **Ground Truth:** By heat shock at 50 degrees Celsius.
- **Instruction:** What are the environmental factors that induce the expression of <protein>? (P83404)
  - **Response:** By bacterial infection.
  - **Ground Truth:** By bacterial and parasitic hemolymph and gut infections.
- **Instruction:** What environmental factors causes the upregulation of <protein>? (D2TDA7)
  - **Response:** By DNA damage, as part of the SOS response.
  - **Ground Truth:** By DNA damage, as part of the SOS response.

#### Molecular Function/Biological Process/Cellular Component (Gene Ontology)

- **Instruction:** Which GO molecular function terms have <protein> been assigned to? (Q7VY99)
  - **Response:** transaldolase activity
  - **Ground Truth:** transaldolase activity
- **Instruction:** What biological process is associated with <protein>? (Q6PDU1)
  - **Response:** mRNA processing; regulation of alternative mRNA splicing, via spliceosome; RNA splicing
  - **Ground Truth:** mRNA splicing; regulation of alternative mRNA splicing, via spliceosome; response to vitamin E
- **Instruction:** Which GO terms outline the cellular components of <protein>? (F4HZB9)
  - **Response:** plasma membrane; side of membrane
  - **Ground Truth:** plasma membrane; side of membrane

#### Short Sequence Motif

- **Instruction:** Can you identify and list all the motifs that are predicted to be present in <protein>? (Q83I16)
  - **Response:** 'HIGH' region; 'KMSKS' region
  - **Ground Truth:** 'HIGH' region; 'KMSKS' region
- **Instruction:** What are the short sequence motifs that are predicted to be present in <protein>? (Q5R4H0)
  - **Response:** LXXLL motif; Methionine segments (Mets) motif
  - **Ground Truth:** LXXLL motif
- **Instruction:** What are the short sequence motifs that are present in <protein>? (B7H6M7)
  - **Response:** PRPP-binding
  - **Ground Truth:** PRPP-binding

#### Tissue Specificity

- **Instruction:** In which tissues is the expression of <protein> absent? (Q5XIJ5)
  - **Response:** Expressed in brain (at protein level).
  - **Ground Truth:** Expressed in brain (at protein level). Expressed in hippocampal neurons.
- **Instruction:** Describe the tissue-specific expression pattern of <protein>? (Q6R2K3)
  - **Response:** Expressed in roots, leaves, stems, flowers and siliques.
  - **Ground Truth:** Expressed in seedlings, roots, stems, leaves, flowers and siliques.
- **Instruction:** What is the tissue-specific expression pattern of <protein>? (C0HJA8)
  - **Response:** Expressed by the venom duct.

- **Ground Truth:** Expressed by venom duct.

#### Activity Regulation

- **Instruction:** Describe the activity regulatory mechanism of <protein> associated enzymes, transporters, microbial transcription factors. (A3MKU1)
  - **Response:** Activated by UTP.
  - **Ground Truth:** Inhibited by UTP.
- **Instruction:** What is the activity regulatory mechanism of <protein>? (Q9US43)
  - **Response:** Allosterically activated by GTP.
  - **Ground Truth:** Allosterically activated by GTP.
- **Instruction:** Tell me about the activity regulatory mechanism of <protein>. (Q63486)
  - **Response:** The activation of GTP-binding proteins is generally mediated by a guanine exchange factor (GEF), while inactivation through hydrolysis of bound GTP is catalyzed by a GTPase activating protein (GAP).
  - **Ground Truth:** The activation of GTP-binding proteins is generally mediated by a guanine exchange factor (GEF), while inactivation through hydrolysis of bound GTP is catalyzed by a GTPase activating protein (GAP). The Ragulator complex functions as a GEF and promotes the active GTP-bound form. The GATOR1 complex functions as a GAP and stimulates RRAGA GTPase activity to turn it into its inactive GDP-bound form, preventing mTORC1 recruitment and activation.

#### Pathway

- **Instruction:** What is the role of <protein> in the metabolic pathway? (Q6MUA3)
  - **Response:** Pyrimidine metabolism; CTP biosynthesis via de novo pathway; CTP from UDP: step 2/2.
  - **Ground Truth:** Pyrimidine metabolism; CTP biosynthesis via de novo pathway; CTP from UDP: step 2/2.
- **Instruction:** Which metabolic pathway does <protein> associate with? (Q63AF7)
  - **Response:** Carbohydrate degradation; pentose phosphate pathway; D-ribose 5-phosphate from D-ribulose 5-phosphate (non-oxidative stage): step 1/1.
  - **Ground Truth:** Carbohydrate degradation; pentose phosphate pathway; D-ribose 5-phosphate from D-ribulose 5-phosphate (non-oxidative stage): step 1/1.
- **Instruction:** What is the metabolic pathway that <protein> is involved in? (Q9SIB9)
  - **Response:** Carbohydrate metabolism; tricarboxylic acid cycle; isocitrate from oxaloacetate: step 2/2; Organic acid metabolism; propanoate degradation.
  - **Ground Truth:** Carbohydrate metabolism; tricarboxylic acid cycle; isocitrate from oxaloacetate: step 2/2.

Subsequently, based on the above cases, we present the error patterns observed for each question type, with a comprehensive summary below:

- For Function, Similarity, and Subcellular Location properties and functions, our model demonstrates high prediction accuracy due to comprehensive annotation coverage and standardized formats.

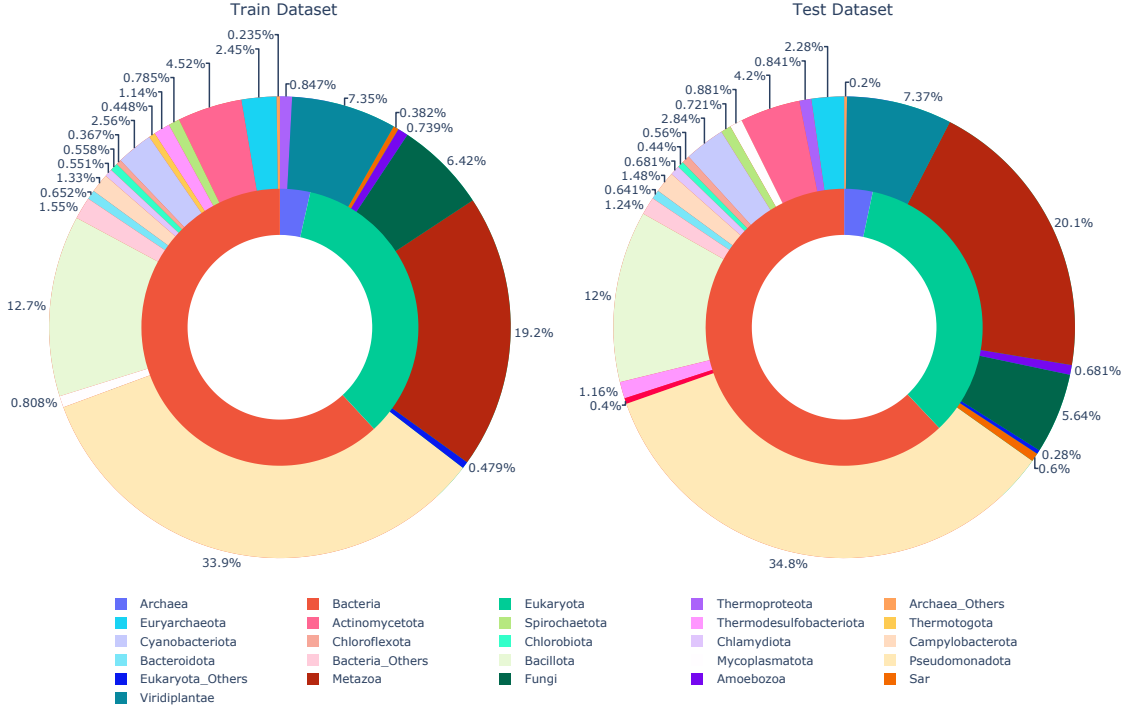


Figure 7: Taxonomic distribution at kingdom and phylum levels in open-ended generation dataset.

- Regarding the three Gene Ontology-related properties and functions, the model achieves accurate predictions for the majority of proteins, with primary errors manifesting as either under-prediction or over-prediction of certain terms.
- For other properties and functions with adequate annotation coverage (including Induction, Short Sequence Motif, Tissue Specificity, Activity Regulation, and Pathway), the model maintains prediction accuracy, with the predominant error being term omission.
- In the case of Developmental Stage, which suffers from limited annotation coverage and poor standardization, while the model may not achieve perfect annotation accuracy, it successfully captures the essential meaning, as illustrated in this example:
  - Instruction:** At which specific developmental stages is <protein> expressed? (A5HEI1)
  - **Response:** Expressed in **embryos** (at protein level).
  - **Ground Truth:** Detected throughout the **embryo**, covering all stages of development from pre-globular to torpedo stages.

**Analysis Based on Taxonomic Classification.** Using the open-ended generation dataset as an example, we show the distribution of kingdom and phylum in the training and test sets in Figure 7. Additionally, in Table 15, we present the performance of SEPIT-TinyLlama-MoEs across different kingdoms on the OOD proteins (considering annotation coverage differences across kingdoms, we selected the 3 most comprehensively annotated properties and

Table 15: Performance comparison of SEPIT-TinyLlama-MoEs across different kingdoms on OOD proteins.

Kingdom	BLEU-2	ROUGE-1	ROUGE-L	METEOR	BERT-F1
Archaea	64.14	68.82	68.32	67.32	95.35
Bacteria	64.73	72.17	71.16	69.75	95.69
Eukaryota	52.68	61.84	59.84	59.75	94.40

functions: Function, Similarity, and Subcellular location). Intuitively, since *Eukaryota* have significantly more training data compared to *Archaea*, the model would be expected to perform better on eukaryotic proteins. However, contrary to this expectation, *Archaea* and *Bacteria* demonstrate superior performance. We attribute this phenomenon to two primary factors:

- **Data complexity differences:**
  - Although *Eukaryota* has more training data, eukaryotic genomes and protein structures typically exhibit higher complexity.
  - Eukaryotic function descriptions tend to be more elaborate, detailed, and diverse, thereby increasing the complexity of the generation task.
- **Data quality factors:** Despite the larger dataset size for *Eukaryota*, it encompasses more noise and heterogeneous annotations, including a higher prevalence of technical terminology and intricate biological processes, which poses greater challenges for accurate prediction.